FABRICATION AND OPTIMAL-DESIGN OF

BIODEGRADABLE STENTS FOR THE TREATMENT OF ANEURYSMS

A Thesis Submitted to the College of
Graduate Studies and Research
In Partial Fulfillment of the Requirements
For the Degree of Master of Science
In the Department of Mechanical Engineering
University of Saskatchewan
Saskatoon, Saskatchewan
Canada

By

XUE HAN

PERMISSION TO USE

In presenting this thesis in partial fulfillment of the requirements for a Master of Science degree from the University of Saskatchewan, the author agrees that the Libraries of this University may make it freely available for inspection. The author further agrees that permission for copying of this thesis in any manner, in whole or in part, for scholarly purposes may be granted by the professor or professors who supervised the thesis work or, in their absence, by the Head of the Department or the Dean of the College in which the thesis work was done. It is understood that any copying or publication or use of this thesis or parts thereof for financial gain shall not be allowed without the author's written permission. It is also understood that due recognition shall be given to the author and to the University of Saskatchewan in any scholarly use which may be made of any material in this thesis.

Requests for permission to copy or to make other use of material in this thesis in whole or part should be addressed to:

Head of the Department of Mechanical Engineering

University of Saskatchewan

57 Campus Drive, Saskatoon, Saskatchewan S7N 5A9 CANADA

ABSTRACT

An aneurysm is a balloon-like bulge in the wall of blood vessels, occurring in major arteries from the heart and brain. Biodegradable stent-assisted coiling is expected to be the ideal treatment of wide-neck complex aneurysms. A number of biodegradable stents are promising, but also with issues and/or several limitations to be addressed. From the design point of view, biodegradable stents are typically designed without structure optimization. The drawbacks of these stents often cause weaker mechanical properties than native arterial vessels. From the fabrication point of view, the conventional methods of the fabricating stent are time-consuming and expensive, and also lack precise control over the stent microstructure. As an emerging fabrication technique, dispensing-based rapid prototyping (DBRP) allows for more accurate control over the scaffold microstructure, thus facilitating the fabrication of stents as designed.

This thesis is aimed at developing methods for fabrication and optimal design of biodegradable stents for treating aneurysms. Firstly, a method was developed to fabricate biodegradable stents by using the DBRP technique. Then, a compression test was carried out to characterize the radial deformation of the stents fabricated. The results illustrated the stent with a zigzag structure has a higher radial stiffness than the one with a coil structure. On this basis, the stent with a zigzag structure was chosen to develop a finite element model for simulating the real compression tests. The result showed the finite element model of biodegradable stents is acceptable within a range of radial deformation around 20%. Furthermore, an optimization of the zigzag structure was performed with ANSYS DesignXplorer, and the results indicated that the total deformation could be decreased by 35% by optimizing the structure parameters, which would represent a significant advance of the radial stiffness of biodegradable stents. Finally, the optimized stent was used to investigate its deformation in a blood vessel. The deformation is found to be 0.25 mm in the simulation, and the rigidity of biodegradable stents is 7.22%, which is able

to support the blood vessel all. It is illustrated that the finite element analysis indeed helps in designing stents with new structures and therefore improved mechanical properties.

ACKNOWLEDGEMENTS

I am heartily thankful to my supervisors, Drs. Daniel Chen and Michael Kelly, for their encouragement, guidance and support through my study program. Their expertise and enthusiasm inspired me to explore and overcome the challenges. I will always be grateful.

I also would like to extend my appreciation to the members of my Advisory Committee, Drs. Qiaoqin Yang and Allan Dolovich for their examination and advices in my research program.

Special thanks are due to my friends for their help and support during my research. They are Dr. Ning Zhu, Dr. Zohreh Izadifar, Ms. Jingwen Li, Dr. Jingyang Peng, and Dr. Chunzi Zhang.

Finally, I gratefully acknowledge the financial support from the China Scholarship Council (CSC).

TABLE OF CONTENTS

LIST OF TABLES

LIST OF FIGURES

LIST OF ABBREVIATION

BDS	Biodegradable stents
BVS	Bioresorbable Vascular Scaffold
DBRP	Dispensing-based rapid prototyping
DES	Drug-eluting stents
EVT	Endovascular treatment
FDM	Fused deposition molding
ICM	Injection and compression molding
ISR	In-stent restenosis
PCL	Poly (caprolactone)
PDLA	Poly (D-lactide)
PDLLA	Poly (D-L-lactide)
PGA	Polyglycolic acid
PLLA	Poly-l-lactic acid
PLA	Polylactic acid
SAC	Stent-assisted coiling

CHAPTER 1 Introduction

1.1 Research Background and Motivation

An aneurysm is a balloon-like bulge in the wall of blood vessels, occurring in major arteries from the heart (aortic aneurysm) and brain (cerebral aneurysm). Aortic aneurysms cause over 13,000 deaths in America each year [1], and cerebral aneurysms contribute to approximately 30,000 people suffering a rupture in America each year [2]. When an intracranial aneurysm ruptures, it may bleed into the subarachnoid space and result in a subarachnoid hemorrhage, with a mortality rate of 25% to 50% [2]. Endovascular treatment (EVT) by selective coiling is considered one of the main treatments for intracranial aneurysms. The efficacy of EVT is limited with respect to the treatment of wide-necked and/or large aneurysms and recanalization can occur after EVT. To circumvent these limitations, a number of new devices have been developed over the last decade. [3] Among them, self-expandable stents made from biodegradable material are promising, and can provide temporary scaffolds in the blood vessel.

Over the past two decades, metallic stents have been considered the gold standard in terms of treatment of more complex intracranial aneurysms. Recently, biodegradable stents (BDS) have been emerging and demonstrating advantages over permanent metallic stents [4]. First, the option of BDS may alleviate patient concerns over permanent implants, especially with respect to the possibility of late stent thrombosis and in-stent stenosis [5]. Second, BDS can help to control drug release and can facilitate the reduction of in-stent neointimal formation and consequently minimize the circumstance of restenosis [6]. With the degradation of the stents, only is a healed arterial vessel left behind. Therefore, long-term clinical problems such as in-stent restenosis and late stent thrombosis could be solved [7].

1.2 Brief Review of the Related Studies

Recently, the research on degradable biomaterials has become one of the most revolutionary studies at the forefront of biomaterials. This novel class of biomaterial is expected to serve as temporary implants, such as scaffolds and stents. The biodegradable stent is able to provide a temporary support to a blood vessel, and then to be dissolved progressively afterwards [7].

Stack et al. at Duke University developed the first biodegradable stents and implanted them in animals [8]. A polymer monofilament of poly-L-lactic acid (PLLA) was used for this prototype stent, which could keep its radial strength for 1 month with up to 1000 mm Hg of crush pressure. It took 9 months for the stent to be almost completely degraded. Clinical results remained limited despite the presence of moderate neointimal growth, minimal thrombosis and a limited inflammatory response in early animal implants.

The Igaki-Tamai stent, the first bioabsorbable stent, was implanted in humans. The Igaki-Tamai stent is made of PLLA with a thickness of 170 μm with a zigzag helical coil pattern. However, the Igaki-Tamai stent lacked a drug coating, which limited its development. The study [9] shows the comparison of the results between the Igaki-Tamai and the metal stents. The Igaki-Tamai stent achieved a high secondary patency rate after a year, but the modifications of stent characteristics are needed with the goal to decrease the restenosis rate during the reabsorption period.

The leading effort in this area in the market is sponsored by Abbott Laboratories, which has been developing a new type of stent called Absorb. Absorb is made of PLLA with a Poly (D-L-lactide) (PDLLA) coating. The diameter of Absorb is from 2.5 mm to 3.5 mm, and the length is from 8mm to 28mm with the thickness of 150 μm strut in the form of zig-zag hoops. The Absorb stent is able to deliver drugs to reduce inflammatory reaction [10].

1.3 Research Issues and Objectives

Currently, there are a number of biodegradable polymeric stents that have shown some successes, but also, with issues and/or several limitations to be addressed. Most biodegradable stents are made with zigzag structures, but there is no optimal design method utilized, drawbacks of which often cause weaker mechanical properties compared to native arterial vessels and result in early recoil post implantation [11]. In addition, the conventional methods of fabricating stents are typical to braid monofilaments of biodegradable polymer into a tubular structure [12, 13], thus being time-consuming and expensive, and also lack precise control over the stent microstructure. Therefore, the conventional methods of fabricating stents result in poor repeatability and limit the design improvements that can be made. As an emerging fabrication technique, the dispensing-based rapid prototyping (DBRP) allows for more accurate control over the scaffold microstructure, thus facilitating the fabrication of stents as designed [14, 15].

The present research is aimed at developing methods for fabrication and optimal design of biodegradable stents for the treatment of aneurysms. The central hypothesis of this research is that *biodegradable stents can be fabricated with a well-controlled microstructure by means of the DBRP fabrication technique, thus providing appropriate mechanical properties for the treatment of aneurysms.*

The following specific objectives will be pursued in the present research.

1. To develop a method to fabricate the biodegradable stents based on the DBRP techniques;
2. To characterize radial stiffness of the biodegradable stents through compression tests;
3. To model and simulate the compression test of biodegradable stents with Pro/Engineering and ANSYS Workbench software;
4. To optimize the structure of biodegradable stents and to perform a simulation in order to investigate the deformation of biodegradable stents in blood vessels with ANSYS Workbench.

1.4 Outline of the Thesis

The remainder of this thesis is laid out in six chapters as follows:

Chapter 2 presents a literature review on the structures, materials and fabrication techniques of biodegradable stents with their advantages and disadvantages discussed.

Chapter 3 presents a fabrication technique for designed biodegradable stents. This chapter presents the work towards Objective 1.

Chapter 4 documents a study of compression test of biodegradable stents, which aims to achieve Objective 2. Particularly, this chapter includes design and procedure of experiments and discussion of the results.

Chapter 5 presents the development of a parametric model for biodegradable stents and simulation results of compression tests based on the developed model. This chapter presents the work towards Objective 3. In particular, this chapter includes a comparison between the compression test and simulation results to verify the effectiveness of the developed model.

Chapter 6 presents the study on optimizing the structure of biodegradable stents through the ANSYS DesignXplorer, which is a design optimization application that works under the ANSYS Workbench environment. Then, the deformation of the optimized stent in a blood vessel is examined. This chapter is to achieve the Objective 4.

Chapter 7 presents the conclusions drawn from this research, followed by limitations and possible future work.

CHAPTER 2 Literature Review

2.1 Introduction to the Development of Stents for Aneurysm Treatment

An aneurysm is a balloon-like bulge in the wall of blood vessels, occurring in major arteries from the heart and brain. Coiling, one of the main treatments for intracranial aneurysms, is limited with the respect to the treatment of wide-necked and/or large aneurysms. Stent-assisted coiling (SAC) was introduced over 10 years to overcome this challenge [16]. The intracranial stents enabled the endovascular treatment of wide-neck complex aneurysms that cannot be coiled previously. The reason is that stents can prevent coil protrusion into the parent artery and provide a scaffold for endothelial growth and vessel wall healing [17]. It has been proven that SAC is an effective and safe approach through several studies since 1990s [18].

Initially, stents were made of metals such as cobalt-chromium and 316L stainless steel. But some issues including stent thrombosis and in-stent restenosis (ISR) remains to be addressed. Stent thrombosis remains a major cause of death and morbidity after percutaneous interventions, while symptoms of ISR, such as asymptomatic angiographic narrowing and recurrent angina/ischemia, typically occur within 6 to 9 months following intervention [19]. In order to reduce the rate of thrombosis and restenosis, drug-eluting stents (DES) were introduced into clinical practice for the treatment of cardiovascular and cerebral artery disease. However, a limited amount of drug can be carried with the thin polymer coating, thus making it difficult to sustain high local drug concentration for a long period [20]. Due to limitations of bare metallic stents and DES mentioned above, biodegradable stents have the advantage of no longer being present as a foreign material in arteries with their degradation. The other significant advantage is that drugs can be incorporated within stents and then be released in a controlled manner. There has therefore been substantial interest and development in recent years in the field of biodegradable stents.

2.2 Materials for Stents

Biodegradable stents are commonly made from synthetic polymers, because of their broad range of properties [21]. Among them, the mechanical properties, mainly characterized by the radial stiffness, and biodegradability, are of significant importance and should be selected such that biodegradable stents are mechanically strong enough to avoid potential immediate recoil. Once the biodegradable stents are implanted into the blood vessel, mechanical properties must

match the application and maintain sufficiently strong until the surrounding tissue has been healed. It is noted that with the degradation of the polymers, there will be a corresponding change in the mechanical properties of stents, depending on the polymer and manufacturing process of the stents [22]. In addition, there should be nontoxic responses in the body when biodegradable stents, once implanted, are undergoing change through metabolism. Their by-products of biodegradation can be either into the metabolic cycle of the body or extruded outside the body. Finally, the polymers are able to transfer and release drugs into the blood vessel. The polymers for use in biomedical engineering, as reported in the literature, include poly (L-lactide) (PLLA), polyglycolic acid (PGA), poly(D-lactide) (PDLA), Polylactic acid (PLA) and poly (caprolactone) (PCL). Table 1 lists these biodegradable polymers and their properties important in the present research.

Table 1 Biodegradable polymers used for stents

Polymers	Melting Point ((℃)	Modulus (Gpa)	Degradation time (Months)	Biocompatibility	Apply before	References
PLLA	173-178	2.7	＞24	Good	Stent	[20, 21]
PGA	225-178	7.0	6-12	Mild inflammatory		[20]
PDLA	Amorphous	1.9	12-16		Coating	[20]
PLA	180-220	3.2	6-12	No severe inflammatory	Coating	[22]
PCL	59-64	0.4	＞24	good	Stent and Coating	[20,23]

PLA has been clinically used as a biomaterial for scaffold fabricated in tissue engineering, but difficulties in substituting the mechanical properties of metallic stents and destructive inflammatory reactions during polymers erosion leading to in-stent restenosis [24]. By comparison, an advantage of PLLA over other biomaterials is that it possesses high strength in mechanical property listed in table 1. However, PLLA degrades at a low rate due to being more hydrophobic than other biomaterials. It has been presented that high molecular weight PLLA can be absorbed totally in between 2 and 5 years in vivo [25]. Unlike PLLA absorbed slowly, PGA can be absorbed within approximately 6-12 months post-implantation because of greater hydrolytic susceptibility

[26]. A drawback of PGA stents is a lack of pliability. The Kyoto University reported that he PGA coil stent exhibited thrombus deposition in canine implant studies [27]. PDLA and PLA, similar with PLLA, have less strength than PGA.

PCL has an extremely high elongation with low tensile strength, and extensive research focuses on developing various micro-and nano-sized drug-delivery vehicles based on PCL, which is promising to hold and release drugs. PCL is a hydrophobic, semi-crystalline polymer [28]; it is potential shape memory polymer with the ability to return from a deformed state to their original shape by temperature change. Shape memory materials are introduced for cardiovascular stents based on their self-expansion ability. Ajili et al. [29] have recommended a polyurethane/PCL blend material for shape memory stents. Polyurethane compound builded on poly (ε-caprolactone) diol was melt mixed with PCL in four different ratios (20, 30, 40 and 50 wt. %) and their shape memory behaviors were studied. The shape memory effects with recovery temperatures of around the melting temperature of PCL appears in all blends but Polyurethane/PCL (80/20). This study also evaluated the biocompatibility of Polyurethane/PCL (70/30) blend with human bone marrow mesenchymal stem cells. The results presented that the blend is good for cell adhesion and proliferation, which showed good biocompatibility and recommended that this blend might be a material for stent implant in the future. Based on good biocompatibility and moderate mechanical property, PCL has been chosen for the material of biodegradable stents in this project.

2.3 Stents Structures

Stent structure plays a pivotal role in the functionality of a vascular stent. Several criteria should be considered when designing structure of stents. First, stents need appropriate mechanical properties, such as the sufficient circumferential and radial stiffness to withstand the inward radial loading imposed on it by the surrounding vessel, while the device must simultaneously exhibit sufficient flexibility of its major axis to enable location within the curved geometry of the recipient's vessel. Second, the stent surface coverage should also be minimized to lower the risks of thrombosis and neointimal hyperplasia [30]. Typically, stent structures can be divided into two types; one is the coil design and the other is the zigzag design.

2.3.1 Coil structure of biodegradable stents

The coil biodegradable stents are usually constructed of polymer fibers and spring-like support structure in figure 1 (a), which is relatively easy to fabricate with wrapping polymer fibers

or dispensing systems. The coil stent is the most flexible and conformable, which is the key determinants of stent fracture, and it appears that the more flexible and conformable the stent, the less prone it is to fracture. However, mechanical properties of the coil biodegradable stents are weak, especially radial stiffness. In contrast to the metal wire, a polymer fiber coil stent cannot keep its original shape well with lower mechanical strength [31]. One of coil stents in figure 1(b) is that coils are encased in an envelope allowing the stent to be wound tightly [31]. The envelope includes an extension for each coil of the wire, which extension overlaps the neighboring coil when the stent is tightly wound and undeployed; additionally, it extends between the coil and its neighbor when the stent is deployed and unwound [31].

(a) (b)

Figure 1 Coil stents

2.3.2 Zigzag pattern of biodegradable stents

Zigzag patterns for biodegradable stents are widely used. A zigzag in Figure 2 is a pattern made up of small corners at variable angles, with a symmetric structure at the peak or valley point. The length of the line connecting peak and valley can be different in order to form a special zigzag pattern [32].

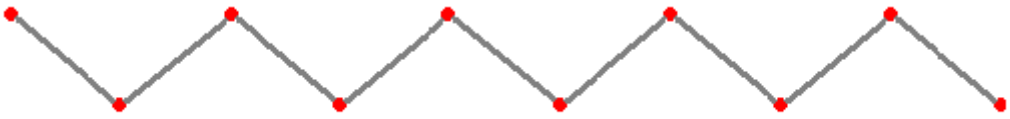

Figure 2 Zigzag pattern

Since a coil stent is made by simply bending a wire having flexibility, the coil stent is expanded not only easily, but also shrunk easily. Namely, the coil stent does not have enough support capability for maintaining the expanded situation in order to hold the body lumen open. On the other hand, a zigzag type stent has enough support capability to retain its expanded situation

for holding the body lumen open. However, since the zigzag stent is not flexible in the axial direction, it is hard to deliver the zigzag stent and to locate the stent in the desirable site [33]. In the zigzag pattern stent, struts attached in zigzag shape are joined in the circumferential direction to form a tubular shape stent. Hence, when the stent is expanded, the struts in the zigzag shape expand in the circumferential direction (Figure 3 [33]).

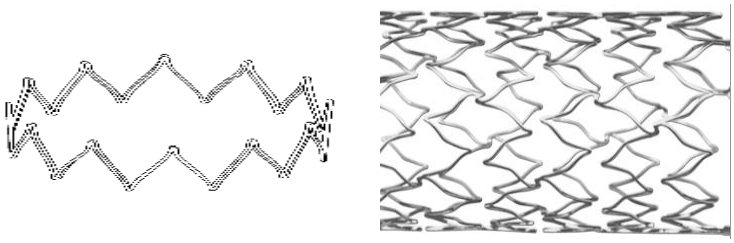

Figure 3 Zigzag stents

2.4 Biodegradable stent products

2.4.1 Igaki-Tamai Stent

The first bioabsorbable stent implanted in humans was the Igaki-Tamai stent (Figure 4), which is formed of high molecular weight (321kDa) biodegradable polymer PLLA [34]. It has a zig-zag helical coils with 0.17mm strut thickness and takes more than three years for complete degradation in the human body. The stent expands by itself with an adequate temperature, and it is without a drug coating. In the study [35], 25 stents were implanted in 19 lesions in 15 patients, and no stent thrombosis and no major cardiac event occurred within 30 days. The study suggests that the Igaki-Tamai stents are feasible, safe, and effective in humans. Long-term investigations with more patients will be required to validate the long-term efficacy of Igaki-Tamai stents.

Figure 4 Igaki-tamai stent

2.4.2 Absorb Bioresorbable Vascular Scaffold

The Absorb Bioresorbable Vascular Scaffold (BVS) (Abbott, Santa Clara, CA) is the most advanced bioresorbable vascular scaffold. BVS is a small mesh tube, made from poly (L-lactide)

(PLLA), and coating with poly (D, L-lactide) (PDLLA) which can help release drugs. The scaffold can be expanded by a balloon and has two platinum radio-opaque markers [36].

The first –in- man trial indicated that the feasibility of the BVS. At 1 year, there were no late stent thromboses. Within 2 years' clinical observation， vasomotion restored and the scaffold was safe without stent thrombosis or cardiac death [37]. Based on ABSORB trails, Abbott made some change to the Absorb BVS concentrated on improving the duration of vessel support without modifying other key design parameters. The product in multiple sizes, including 2.5mm, 3.0mm, and 3.5mm diameters and 12, 18, and 28mm lengths, is available now(Figure 5) [38].

Figure 5 Absorb Bioresorbable Vascular Scaffold

2.4.3 REVA Stent

The first-generation REVA stent (REVA Medical, San Diego, California, United States) is made of a tyrosine-derived poly carbonate without drug- eluting and has a unique side-lock structure with a 0.2mm strut thickness to allow for safe expansion and provides excellent radial stiffness to withstand the redial force (Figure 6). Nevertheless, the results showed that there was a high restenosis rate secondary to focal mechanical failures in the human trial [39]. A redesign, the ReZolve 2 Scaffold, was reformed and is undergoing initial testing. It utilizes an improved tyrosine polycarbonate polymer that provides a 30% increase in radial stiffness [40].

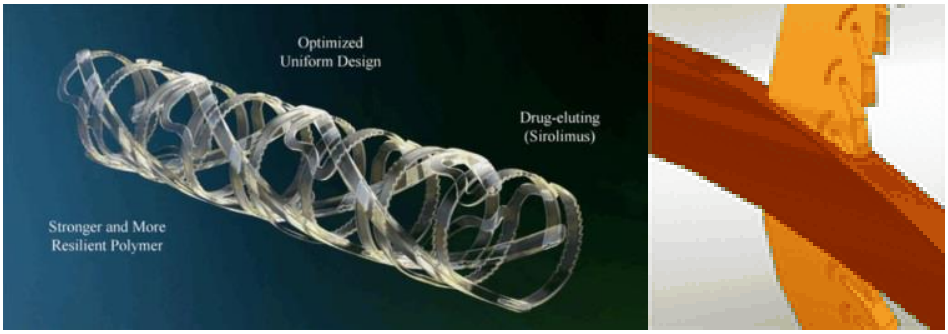

Figure 6 ReZolve Sirolimus-Eluting Bioresorbable Coronary Scaffold with slide and lock mechanism

2.5 Methods for Fabricating Biodegradable Stents

Commonly, there are two types of fabrication methods for stents fabrication. Top-down fabrication approaches, such as laser machining, molding, and electroforming, are subtractive processes starting from bulk materials, while bottom-up fabrication strategies, such as solvent casting and 3dimensional (3D) printing, are additive processes [41]. Applications of both methods to the stent fabrication are briefly reviewed in the following.

Laser machining commonly used stent fabrication process is basically a two-step process, i.e., a polymer tube created and then cut by laser to form stents. Compared to other cutting methods, laser processing produces very smooth edges that substantially reduce the need for finishing the process. The benefit of which is the ability to make intricate design cuts with extreme precision and accuracy. However, this two-step process is time-consuming and not efficient in using biodegradable polymers. Laser machining has been used to produce polymeric stents, such as REVA stents, however, alterations may be made when concerning thermal and chemical polymer properties.

Injection and compression molding processes are particularly appropriate for polymeric materials due to their thermoplastic behavior with recent efforts directed at optimizing micro-and nano-molding processes [41-44]. Injection and compression molding (ICM) combines the techniques of both injection molding and compression molding. In the injection and compression molding process, heat and pressure are exerted on the molding cavity, causing it to solidify into the mold shape [45]. ICM not only keeps the advantages of conventional injection molding but also increases the reproduction of micro-surface feature and reduces flow distance/wall thickness ratio. However, it is not easy for the user to implement ICM process, as the melt penetrating to

the parting line can be caused by late compression while incomplete filling may be caused by early compression.

Fused deposition molding (FDM) consists of repeated deposition of thin layers of polymer and assembling the layers into 3D microstructures [46]. Moreover, *melt spinning* can be used to form bioabsorbable polymer fibers in the range of 150 μm to 200 μm that can then be woven or knitted into stent-like structures [47, 48]. These two fabrication techniques are still in their early stages, and further study is needed. Also, the available materials for FDM are restricted due to the melting points.

3D-Bioplotter has been widely utilized in tissue engineering to fabricate tissue scaffolds by taking advantage of dispensing based rapid prototyping techniques. The benefits include precise control over microstructure, good repeatability, capacity for adapting to different materials states, from liquid to a thick paste, and relatively mild fabrication condition such as low operating temperature, no toxic solvent needed, and fast and efficient material processing [14]. 3D-Bioplotter has evolved into an innovative rapid stent fabrication technology for fabricating biodegradable stents. Through this novel biodegradable stent fabrication system, polymer stents with various patterns can be directly made from polymer powders, such as PCL, PLA, and PLLA. Therefore, this technology has shown sound promising to be able to accelerate the stent product development process.

Based on the discussion above, the advantages and disadvantages of fabrication methods for biodegradable stents are summarized below (Table 2).

Table 2 The advantages and disadvantages of fabrication methods for biodegradable stents

Fabrication	Advantages	Disadvantages
Laser cutting	produce small diameter tube high precision low cost	Heat effects Deposition of the removed material
Injection and compression molding	Fast production Low cost	Second operation Design restrictions
Fused deposition molding	Fast fabrication High precision	Heat effects Noddle diameter limitation
3D-Bioplotter	Precise control Low cost High efficiency	

2.6 Radial stiffness test of stents

Stents with high radial stiffness can help to resist early recoil caused by the artery pressure. The radial stiffness of stents was investigated in [49], aiming to simulate and evaluate the deformation of the stents caused by the artery pressure. The test platform included a Plexiglas cylindrical chamber that can be filled with water for pressure control. Additionally, a transparent polyurethane tube filled with water was used as an interface casing for ensuring uniform pressure applied on the stents, and the inner pressure was remained at the average pressure in the artery (100mmHg). The pressure inside the chamber was controlled by a pressure reducing device and measured, and then the diameter of the stents was measured by graduated ruler. From the measured stent diameters under different pressures, the stent deformation behavior can be characterized.

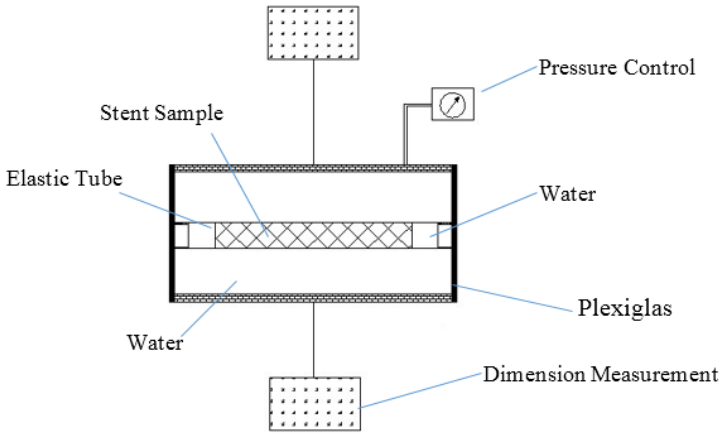

Figure 7 Radial stiffness test platform

2.7 Conclusions

Based on the concept that biomaterials can be degraded, biodegradable stent-assisted coiling is expected to be the ideal treatment of wide-neck complex aneurysms. Currently, there are some products approved for clinical use. Although the short-term results are charming, there are still some concerns such as the weaker mechanical properties of structure and the time-consuming and low-level repeatable fabrication techniques. Therefore, the further studies of structure design and fabrication method are needed. Stent design develops in a manner adopting novel strategies driven by the improvement of material science, microfabrication, and nanotechnology.

CHAPTER 3 Fabrication of Biodegradable Stents

3.1 Fabrication of Stents Based on Rapid Prototyping Dispensing Method

Various rapid prototyping systems have been developed to fabricate scaffolds for tissue engineering, including the biodegradable stents, because rapid prototyping technology not only allows more choice of biomaterials but provides more precise control in the whole fabrication process. Typically, the rapid prototyping system is a computer-controlled three-axis machine with a dispenser head, where the biomaterial in a form of fluid or solution stored a syringe is dispensed out by using air pressure, forming the biodegradable stents while the head is brought to move along three axises.

In the present study, a fluid dispensing equipment (Figure 7) supplied by Nordson Asymtek is used in fabricating biodegradable stents. Through this fluid dispensing equipment, the biodegradable stents can be manufactured with a minimum strand diameter of 0.1 mm. The main parts of the equipment includes a dispensing head, a high-resolution camera, a z-height sensor and a syringe. Specifically, the dispensing head is controlled by high precision motors with a movement resolution of 0.001 mm, and the speed is controlled from 0.1 mm/s to 150 mm/s. Additionally, a high-resolution camera is used for needle tip positioning and strand dimension control. For automatically controlling the height of the head, a z-height sensor is built in. Furthermore, there is a fluid pressure gauge indicating the air pressure supplied to the syringe. The fluid pump dispenses the liquid and is mounted on the dispensing head, and holds the syringe of dispensing fluid.

To fabricate biodegradable stents, a motorized cylindrical substrate (Figure 8) will be used. On the substrate, a replaceable mandrel is connected to the shaft of an electric motor via a spindle; as such the mandrel can be rotated by the electric motor in a controlled manner. Then, the biomaterials can be dispensed onto the surface of the mandrel via the dispensing machine. The fluid dispensing mechanism (Figure 9) is so configured that its dispensing head can move along the mandrel in a controlled manner while distributing the biomaterials onto the top surface of the mandrel at a controllable flow rate. During the fabrication process, the rotational motion of the mandrel and the translational motion of the fluid dispensing head are coordinated such that the fluid dispensing head traces and dispenses biomaterials to the designed location of the strands of the stent being built, thus forming the stent on the surface of the mandrel.

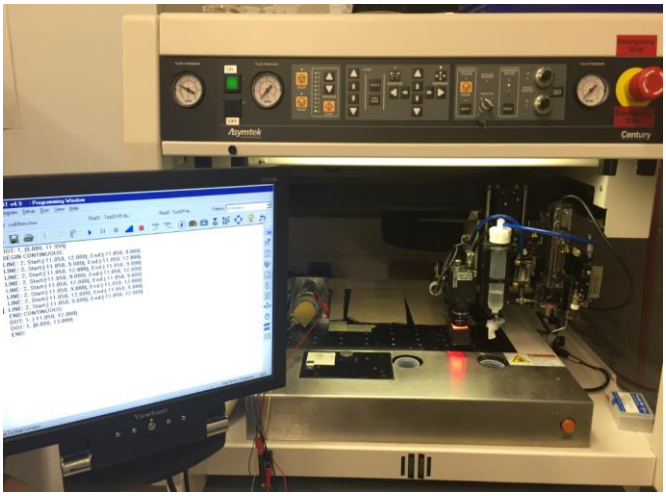

Figure 8 Nordson Asymtek dispensing machine

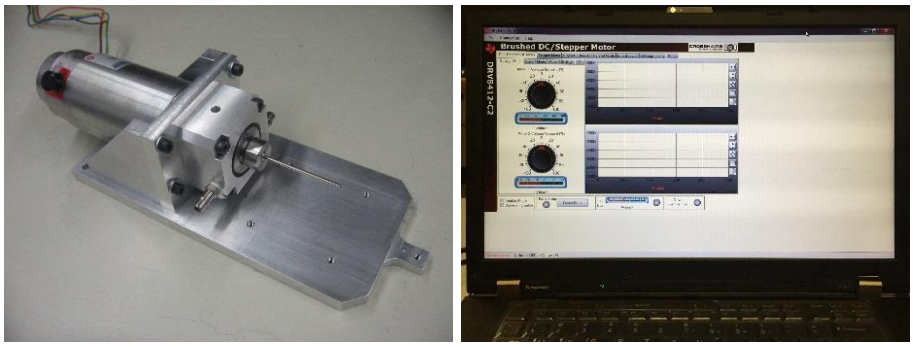

Figure 9 Motorized cylindrical substrate

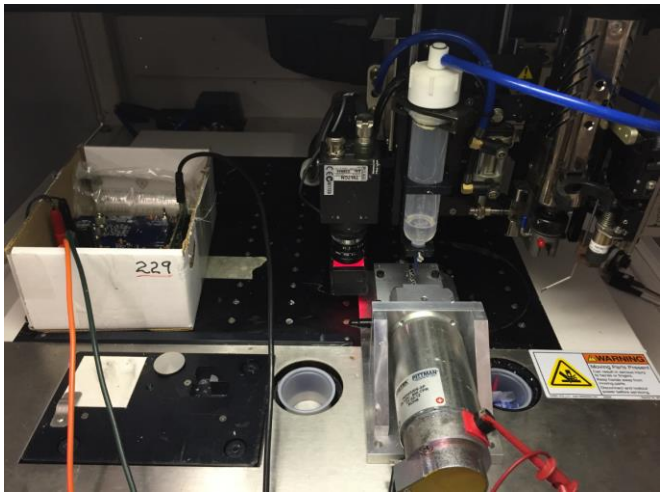

Figure 10 Dispensing mechanism for fabrication biodegradable stents

3.2 Material Preparation and Stent Fabrication

3.2.1 Material Preparation

Polycaprolactone (PCL) powder (MW 50,000) was obtained from Polysciences, Inc. A solvent of chloroform was used, and the concentration of polymer used varied from 50%PCL to 70%PCL. Due to the toxic solvents and the requirement for careful handling, all solutions were prepared under a chemical hood. First the polymer was weighted, 5g, 6g and 7g, for 50%, 60% and 70% concentration solutions respectively, and then put into a glass jar for each one. Subsequently, the chloroform was made in 10ml quantities for each glass jar and added into the glass jar with a stirring rod to obtain a homogeneous solution. The glass jar was then sealed and ready for pouring into a syringe, which was used for dispensing. All solutions were prepared at room temperature.

3.2.2 Stent Fabrication Process

The coil stents and zigzag stents mentioned in chapter 2 will be fabricated in this section, and the fabrication parameters including fluid pressure, dispensing head moving speed, needle size of the dispensing head, mandrel rotating speed and dispensing head height will be investigated.

For achieving the desired accuracy, parameters should be adjusted and matched well. The PCL solution will be dispensed and solidified onto a mandrel, which rotates in a controlled manner, thus forming the structure as shown in a schematic (Figure 10). To accurately deposit the designated material distribution, the flow rate of material and moving speed of the dispensing head will be carefully determined. The flow rate is affected by the concentration of fluids, the needle size of the dispensing head and the air pressure in the syringe. Also, the angular velocity of the mandrel and the moving speed of the dispensing head will be coordinated and programmed to fabricate the coil and zigzag biodegradable stents (Figure 11).

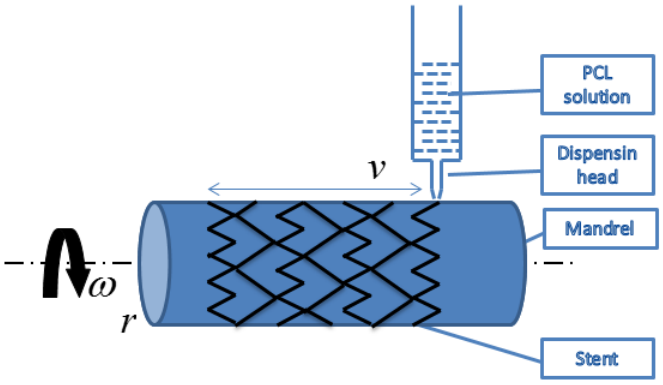

Figure 11 Schematic of fabrication process of biodegradable stents

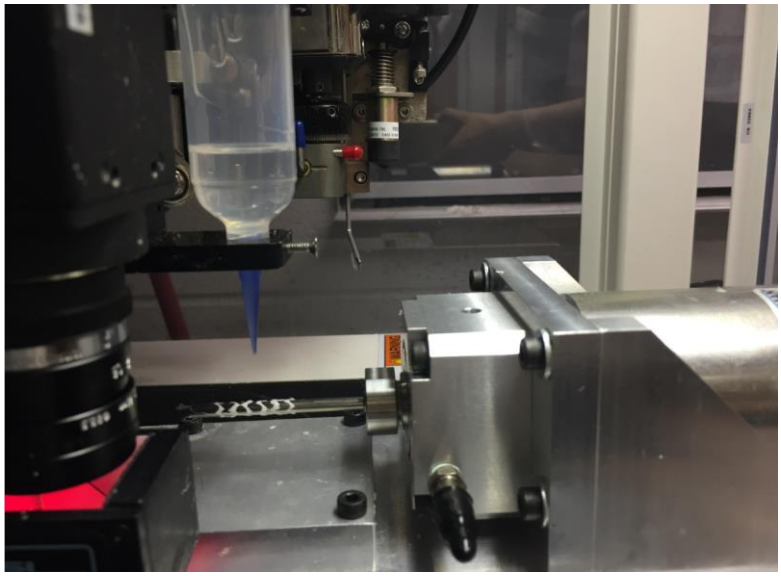

Figure 12 Fabrication process of biodegradable stents

3.3 Characterization of Stents Fabricated

3.3.1 Parameters for Coil Structure with Different Concentration of PCL solution

Working parameters are essential for stents fabrication. Those parameters can be broadly divided into six parts such as the concentration of PCL solution, air pressure, dispensing height, dispensing speed, mandrel rotating speed and diameter of the needle of dispensing head (Table 3).

Table 3 Fabrication parameters for coil structure of biodegradable stents

Coil Structure							
Label	Concentration of PCL solution	Air pressure (psi)	Dispensing height (inch)	Dispensing Speed (Inch/sec)	Mandrel rotating speed (rpm)	Diameter of needle Dispensing head (mm)	Samples
Coil 50	50%PCL	30	1.74	0.7	402	0.25	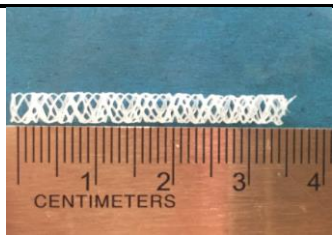
Coil 60	60%PCL	30	1.74	0.7	402	0.41	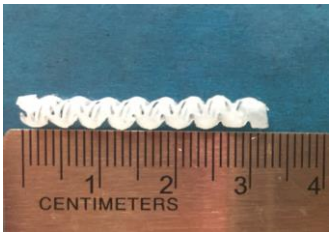
Coil 70	70%PCL	30	1.74	0.7	402	0.41	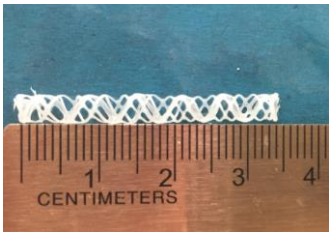

The concentration of PCL solution plays a pivotal role in the coil formation during the fabrication process. Three levels from low to high are utilized in this experiment. As the low concentration leads to the low viscosity, the smaller diameter of the needle for the dispensing head has to be used so that the struts can solidify on the mandrel and not to flow out of the mandrel. 70% PCL solution matches well with the 0.41 mm diameter of the needle for the dispensing head

while the 60% PCL solution cannot form a round strut through 0.41 mm diameter of the needle for the dispensing head because of its low viscosity. Air pressure and dispensing height also have a significant effect on the flow rate of the PCL solution within the syringe. If the flow rate is relatively high or low, the bead strut from the syringe will come out rather than a smooth one. So, the air pressure and dispensing height are adjusted at 30 psi and 1.74 inches respectively for a stable strut. For the coil structure, the mandrel rotating speed has to be relatively high (402 rpm) and the speed of dispensing head is moderate (0.7 inches/sec) to keep an average pitch of the coil structure stents.

3.3.2 Parameters for Zigzag Structure with Different Concentration of PCL solution

There is also three concentration of PCL solutions for fabricating zigzag stents (Table 4).

Table 4 Fabrication parameters for zigzag biodegradable stents

Zigzag Structure							
Label	Concentration of PCL solution	Air pressure (psi)	Dispensing Height (inch)	Dispensing Speed (Inch/sec)	Mandrel rotating speed (rpm)	Diameter of Dispensing head (mm)	Samples
Zigzag50	50%PCL	30	1.74	0.7	232	0.25	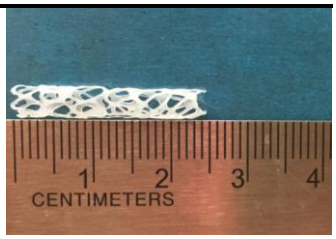
Zigzag60	60%PCL	30	1.74	0.7	232	0.41	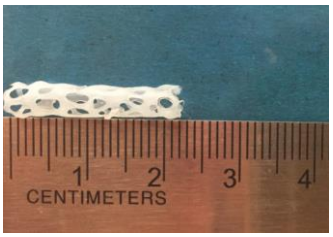
Zigzag70	70%PCL	30	1.74	0.7	232	0.41	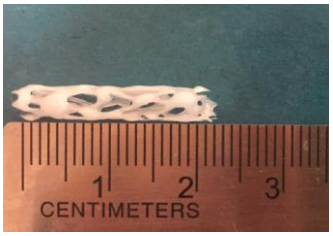

As the same with coil structure, 70% of PCL solution matches the 0.41 mm diameter of the needle for the dispensing head very well, while the 50% PCL solution is suitable for 0.25 mm diameter of the needle for the dispensing head. The air pressure and dispensing height are the same with the values for fabricating the coil structure, as the flow rate is proper for forming the smooth struts. The mandrel rotating speed (232 rpm) in fabricating zigzag structure is much slower than making coil structure because it costs more time for the dispensing head to move forward and back to form a zigzag pattern. The numbers of the zigzag in one row determine the mandrel rotating speed and the speed of dispensing head, which means that the low mandrel rotating speed allows more forward and back movements.

3.3.3 Parameters for Zigzag Structure Made of 70% PCL solution

In order to obtain a zigzag structure with better mechanical property stents, another experiment was carried out to investigate the parameters of fabricating the 70% PCL solution. The speed of dispensing head is the importance of forming a zigzag structure of biodegradable stents, which will be changed from 0.7 to 1.3 inch/sec in this experiment while other parameters keep the same value (Table 5). Through comparison, when the speed of dispensing head is at 0.85 inches/sec, the zigzag structure of biodegradable stent fabricated looks better than others. The property of radial deformation of all of the biodegradable stents was examined by a compression test, as presented in the next chapter.

Table 5 Fabrication parameters for 70% PCL of zigzag biodegradable stents

Zigzag Structure							
Label	Concentration of PCL solution	Air pressure (psi)	Dispensing Height (inch)	Dispensing Speed (Inch/sec)	Mandrel rotating speed (rpm)	Diameter of Dispensing head (mm)	Samples
Zigzag70-0.7	70%PCL	30	1.74	0.7	232	0.41	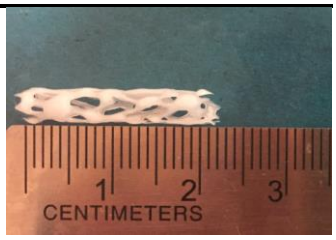
Zigzag70-0.85	70%PCL	30	1.74	0.85	232	0.41	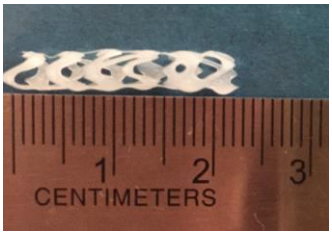
Zigzag70-0.9	70%PCL	30	1.74	0.9	232	0.41	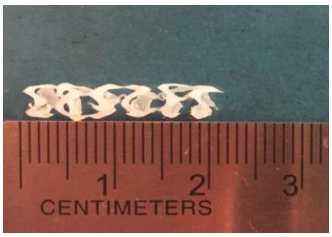
Zigzag70-1.1	70%PCL	30	1.74	1.1	232	0.41	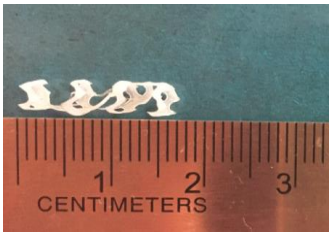
Zigzag70-1.3	70%PCL	30	1.74	1.3	232	0.41	

3.4 Conclusions

This chapter presents the process of fabricating biodegradable stents, and the results show that the dispensing-based rapid prototyping method is a promising technique for fabricating biodegradable stents. With the successful coil and zigzag structures, this method is controllable and able to fabricate more various structures of biodegradable stents.

CHAPTER 4 Compression Test of Biodegradable Stents

4.1 Introduction to the Compression Test System

The radial stiffness, a measurement of the radial rigidity of the biodegradable stents, is of importance for the reduction of target vessel restenosis, as the radial stiffness can present the extent to resist radial deformation of biodegradable stents in response to an applied force [49]. The compression test is an efficient examination method to investigate the radial stiffness of biodegradable stents, which can determine deformation behaviors of biodegradable stents under loads. This chapter is intended to provide a compression comparison of radial deformation among biodegradable stents including coil and zigzag structure fabricated in Chapter 3. Specifically, the biodegradable stents will be compressed, and the displacement at various loads will be recorded.

An advanced design of the Bose Dynamic testing platform to evaluate the deformation of biodegradable stents will be employed (Figure 12), which can provide an accurate characterization of biomaterials and biological samples within a sterile cell culture media environment. Specifically, Bose Dynamic test instruments are integrated systems that combine ElectroForce linear motors with environmental technologies and fully-automated computer control. Proprietary ElectroForce motors provide exceptional fidelity based on their simple and durable moving-magnet design. The Bose Dynamic test instrument is controlled by a PC using Bose PCI digital controls and WinTest software while the WinTest software is an intuitive control system for performing complex test routines with minimal training. Additionally, measurement transducers are provided for each active control channel, including pressure sensors, axial load and displacement measurement.

After loading the sample on the plates, parameters including displacement and compression rate are needed to set for the compression test (Figure 13). In this experiment, the desired displacement is specified manually with a value of -1.8 mm, and the compression rate is set at 0.1mm/sec.

For data acquisition, there are many ways to record data. It is recommended to use timed data from data acquisition tab in the window (Figure 14). The desired measuring time in Scan Time as seconds can be defined. The Scan Points representing the number of data will be acquired in the specified Scan Time. In this experiment, the measured time is 100 s for each stent, and 1000

points are being scanned within 100 s. Then the location and name for the data file can be chosen for saving.

Figure 13 Bose ElectroForce Biodynamic testing system

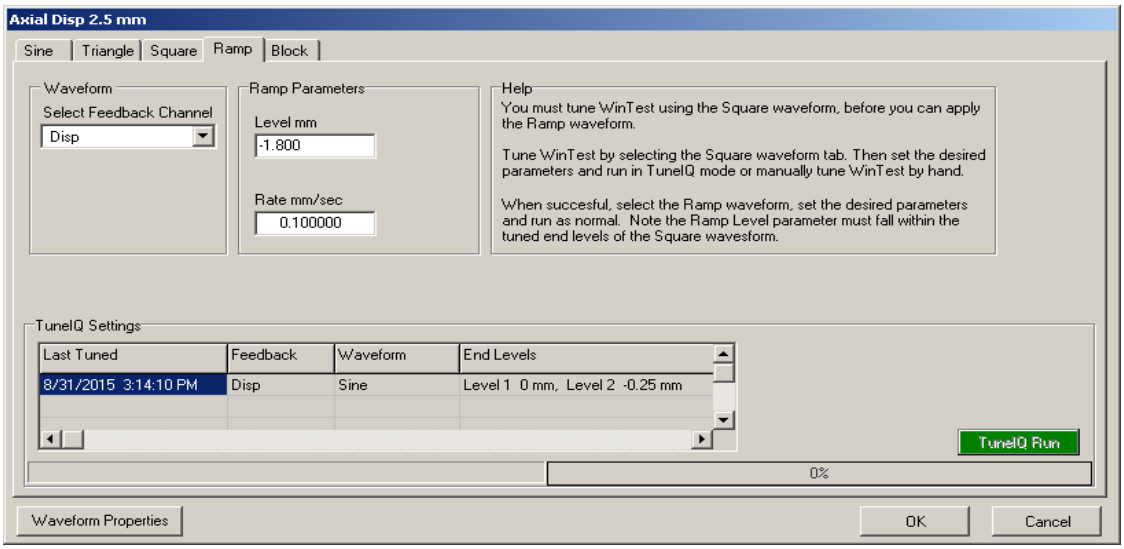

Figure 14 Displacement and compression rate setting

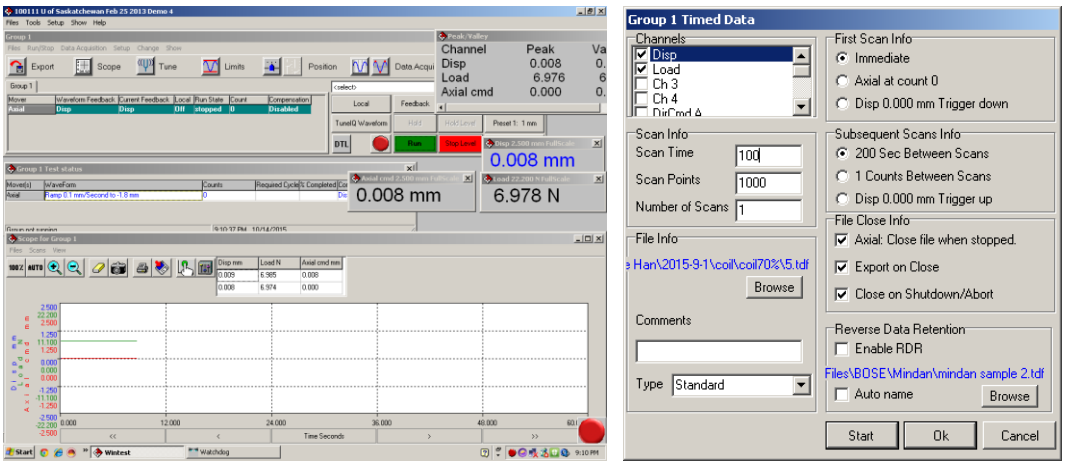

Figure 15 Data acquisition setting

4.2 Experiments Design and Procedure

This experiment aims to determine the deformation of coil and zigzag structure of biodegradable stents under a compressive load through Bose ElectroForce BioDynamic test instrument. During the experiment, loads and displacements are intermittently measured and recorded.

Compression tests are conducted by loading specimen between two plates (Figure 15), and then applying a force to the sample by moving the crossheads underneath. During the test, the biodegradable stents are compressed, and displacements versus the applied loads are recorded.

Figure 16 Loading plates for specimen

The diameter of coil and zigzag structure of biodegradable stents is the same (3.4 mm). The forces required to compress the stents radially by 10% (0.34 mm), 20% (0.68 mm), 30% (1.02

mm) and 40% (1.36 mm) will be measured. Nine groups of biodegradable stents need to be tested, and there are four stents in each group. The letters from A to G are used to represent each group of zigzag biodegradable stents for distinguishing different fabrication parameters and different concentration solution. The concentration of solution of biomaterials is the same (70%) from A to E, while the fabrication parameter (the speed of dispensing head) is different (0.85 inch/sec, 0.7 inch/sec, 0.9 inch/sec, 1.1 inch/sec and 1.3 inch/sec, respectively). F and G represent the 60% and 50% zigzag biodegradable stents when the speed of dispensing head is at 0.7 inch/sec. Coil A and coil B stand for coil structure of biodegradable stents at the concentration of 50% and 70% respectively.

4.3 Testing Results and Discussion

This test examines the following characteristics: radial deformation of biodegradable stents with the compressive force. All the biodegradable stents are compressed in a similar elliptical shape configuration. Comparing with the forces required to compress the biodegradable stents radially by 10%, the largest force is 0.214 N for Group A, and the second one is 0.179 N for Group F. The result means that the zigzag structure in group A can bear more compression forces than other groups and indicates that the zigzag structure in Group A can potentially support the blood vessel in order to make the blood flow fluently (Figure 16).

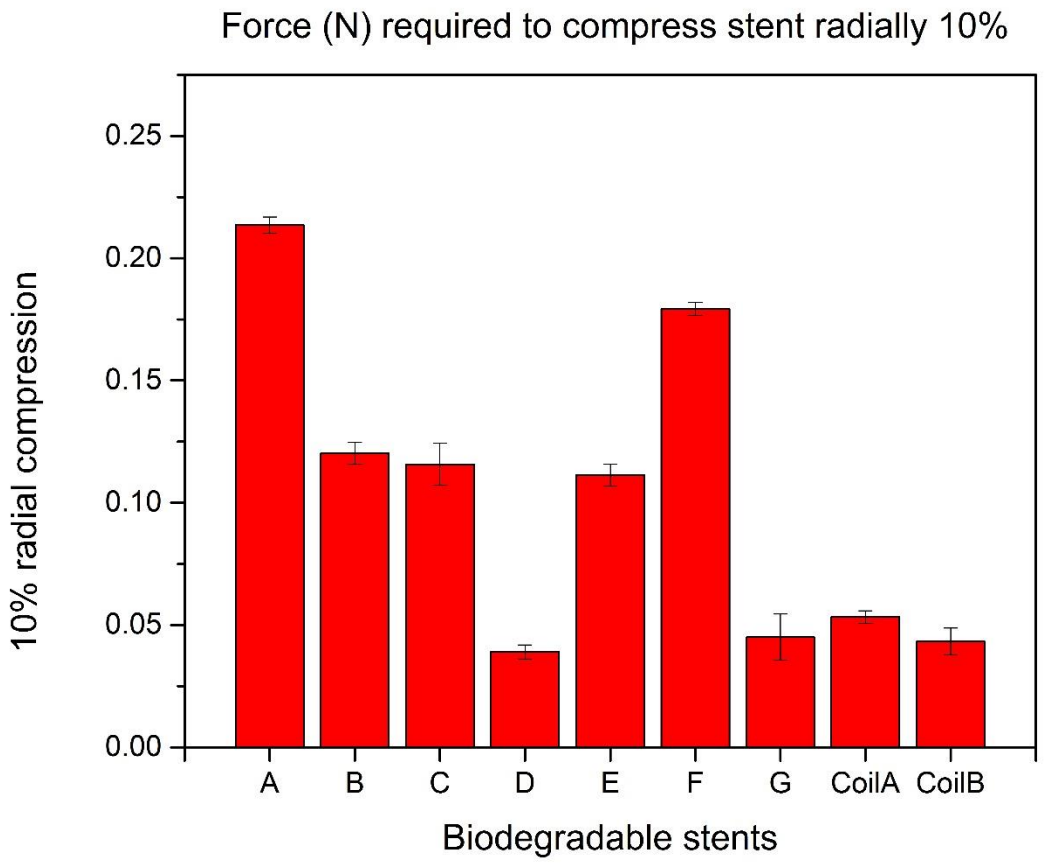

Figure 17 10% radial compression of biodegradable stents

There is no significant difference between the largest force and the second one when compressing the biodegradable stents radially 20%, which are 0.445 N in group A and 0.438 N in Group F respectively (Figure 17).

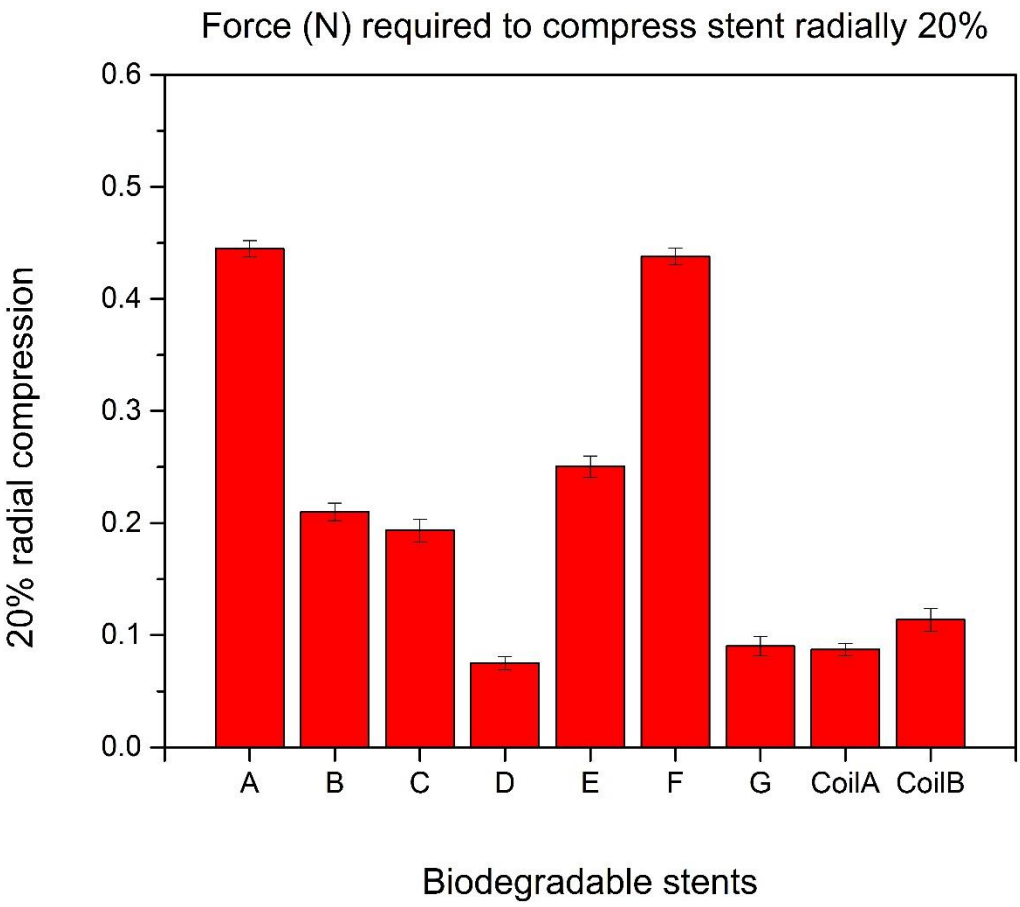

Figure 18 20% radial compression of biodegradable stents

The largest force can compress biodegradable stents radially 30% is 0.813 N in Group A while the second one is 0.713N in Group F (Figure 18).

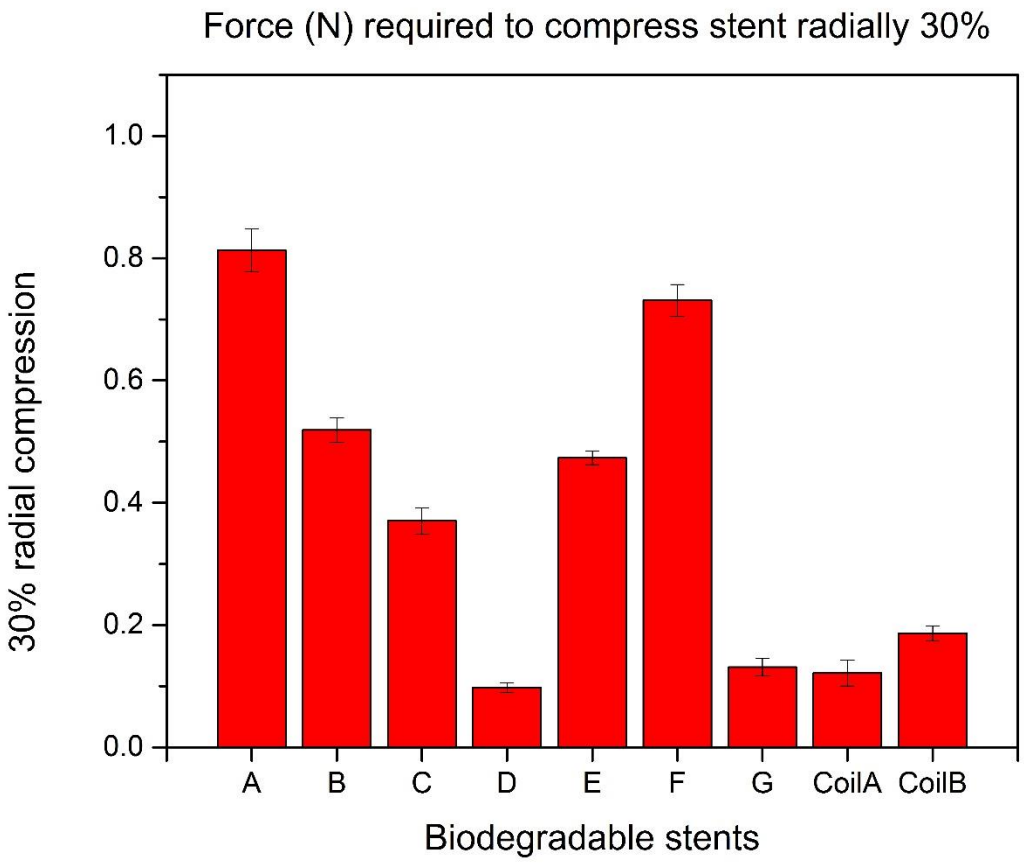

Figure 19 30% radial compression of biodegradable stents

To compress biodegradable stents radially 40%, the force in Group A is 1.342N, with a 27% larger than the second one (Figure 19).

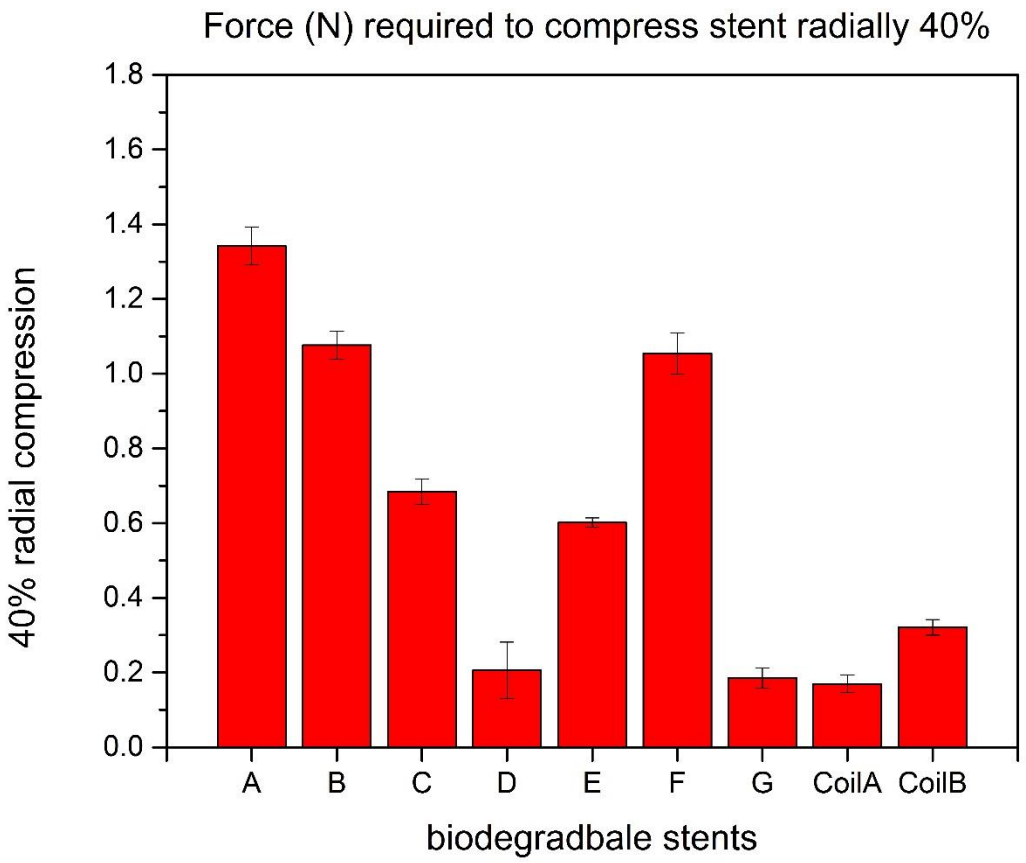

Figure 20 40% radial compression of biodegradable stents

4.4 Conclusions

The compression test results indicate that the radial stiffness of zigzag biodegradable stents is better than the coil stents, and shows the zigzag biodegradable stents in Group A have the highest radial stiffness for bearing compressive forces. The compression test will be modeled and simulated in the next chapter.

CHAPTER 5 Modeling of Biodegradable Stents and Simulation of Compression Test with the Finite Element Analysis Method

5.1 Introduction to Modeling of Biodegradable Stents and Simulation Method with Finite Element Analysis

This chapter presents a parametric design approach to model zigzag structures of biodegradable stents and a finite element analysis method to simulate real compression test of the biodegradable stents performed in Chapter 4.

Solid modeling is a geometrical representation of a real object without losing information which the real object would have. Thus, if the density of the material is given, the mass and inertia of the solid modeling can be calculated with its volume [51]. The solid modeling of biodegradable stents will be built with Pro/Engineer software, which is a feature-based solid modeling tool. Conveniently, each feature can be edited individually and can be changed in the solid modeling. Pro/Engineering is parametric in nature, which means that the characteristics of the part are correlative by taking the reference of each other. It is easy to redefine the dimensions or the attributes of a feature with Pro/Engineer based on the users' requirements, and the changes will be executed automatically throughout modifying the parameters of modeling. The zigzag structure of biodegradable stents is represented by several parameters, and thus, the parametric modeling allows any of the characteristic parameters of the zigzag structure to drive the modification in order to build different models.

The finite element analysis [52] is a numerical method to be applied in structural analysis, solid mechanics and dynamics etc. ANSYS Workbench, a professional tool for the finite element simulation, is the framework combining an industry-leading suite of advanced engineering simulation technology. In the ANSYS Workbench [53], the complex Multiphysics analyzes can be carried out with a simple drag-and-drop through an innovative project schematic. For simulating a compression test, the parametric modeling of biodegradable stents built by Pro/Engineer will be linked into ANSYS Workbench, and a static structural analysis system in ANSYS Workbench will be used to determine the deformation of biodegradable stents under different compression forces.

5.2 Parametric Modeling of Zigzag Structure of Biodegradable Stents

5.2.1 Parameters of biodegradable stents

Based on the biodegradable stents fabricated by the dispensing-based rapid prototyping machine in Chapter 3, the thickness of the strut is 0.41 mm, and the diameter of the stent is 3.4 mm. The model can be built on a flat surface first, and then bended into a tube shape in the Pro/Engineer software. The flat surface of zigzag biodegradable stents can be divided into small cells. There are five zigzag cells in each row along the circumferential direction, and six rows in the axial direction (Figure 20).

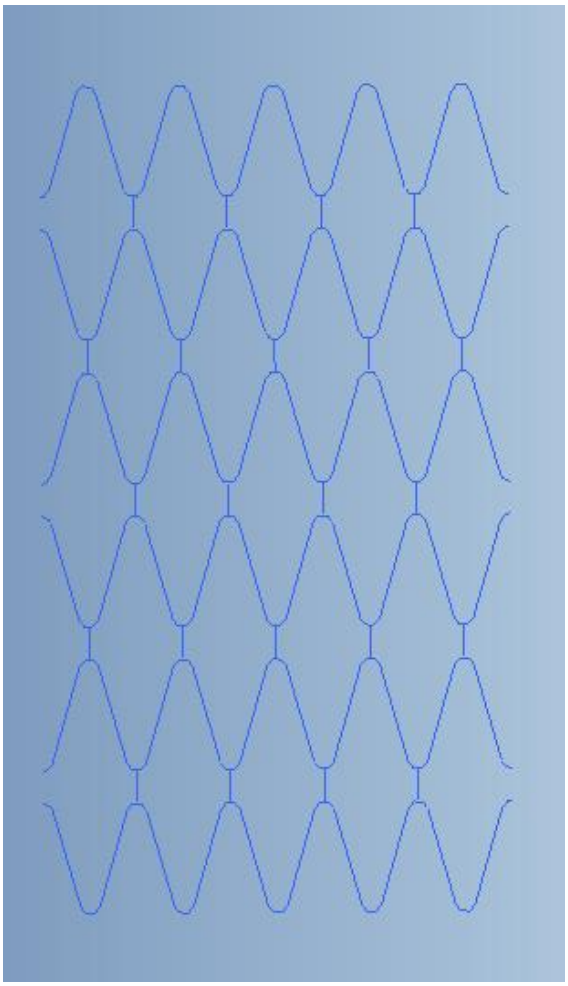

Figure 21 Zigzag pattern of biodegradable stents

There are three parameters to represent a zigzag cell in the axial direction (Figure 21). The one denoted by A in Figure 21 is the diameter of curvature at the apex that is tangential to the line on each side in the circumferential direction. As the diameter of curvature changes, the angle between two lines will be altered. The one denoted by B is the vertical length of the line tangential

with the semi-circle. The one denoted by C is the distance between two apexes of the semi-circles. A new structure can be obtained by changing the size of the parameters. Initially, A is 0.25 mm; B is 2.8 mm and C is 0.8 mm.

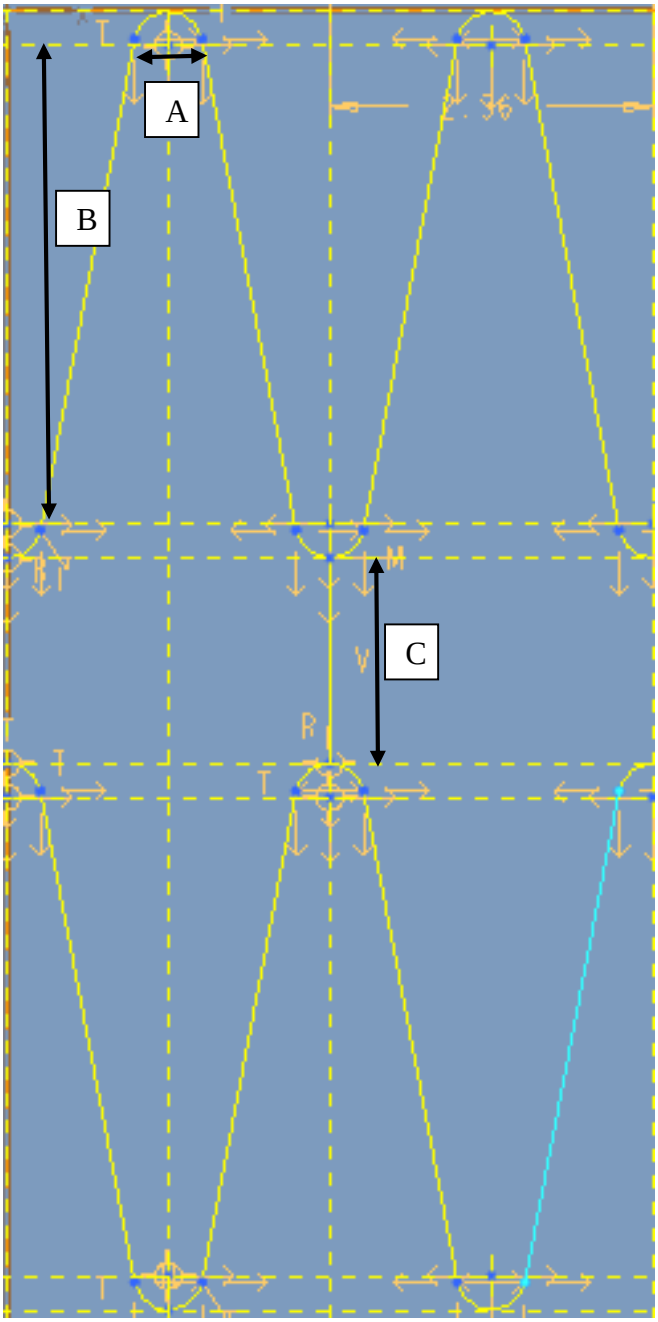

Figure 22 Parameters for each cell of zigzag biodegradable stents

5.2.2 Process of parametric modeling of zigzag biodegradable stents

The process of creating the parametric model of zigzag biodegradable stents with Pro/Engineer software will be introduced in the following.

First, a 2D zigzag structure (Figure 22) can be drawn in the Sketch. The Sketcher toolbar appears to the right of the graphics window. It is convenient to use these Sketcher tools to sketch the curve and a tangential line to form a 2D zigzag structure in the Figure 20.

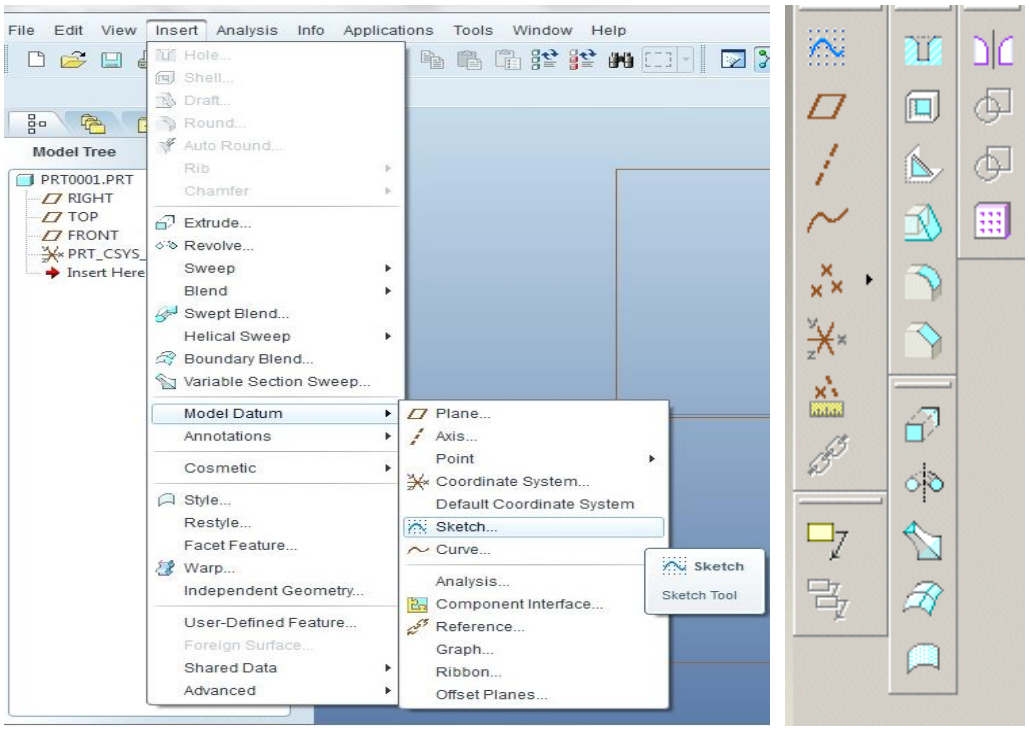

Figure 23 Sketch and tool bar in the Pro/Engineer

Then, a 3D zigzag structure (Figure 23) can be created by a Sweep feature through taking a sketched profile and sweeping it along a selected or sketched trajectory. The cross-section of the feature along the entire length of the trajectory is constant. The cross-section is a circle with 0.41 mm in diameter, which is based on the needle size of the dispensing head used in fabricating the biodegradable stents.

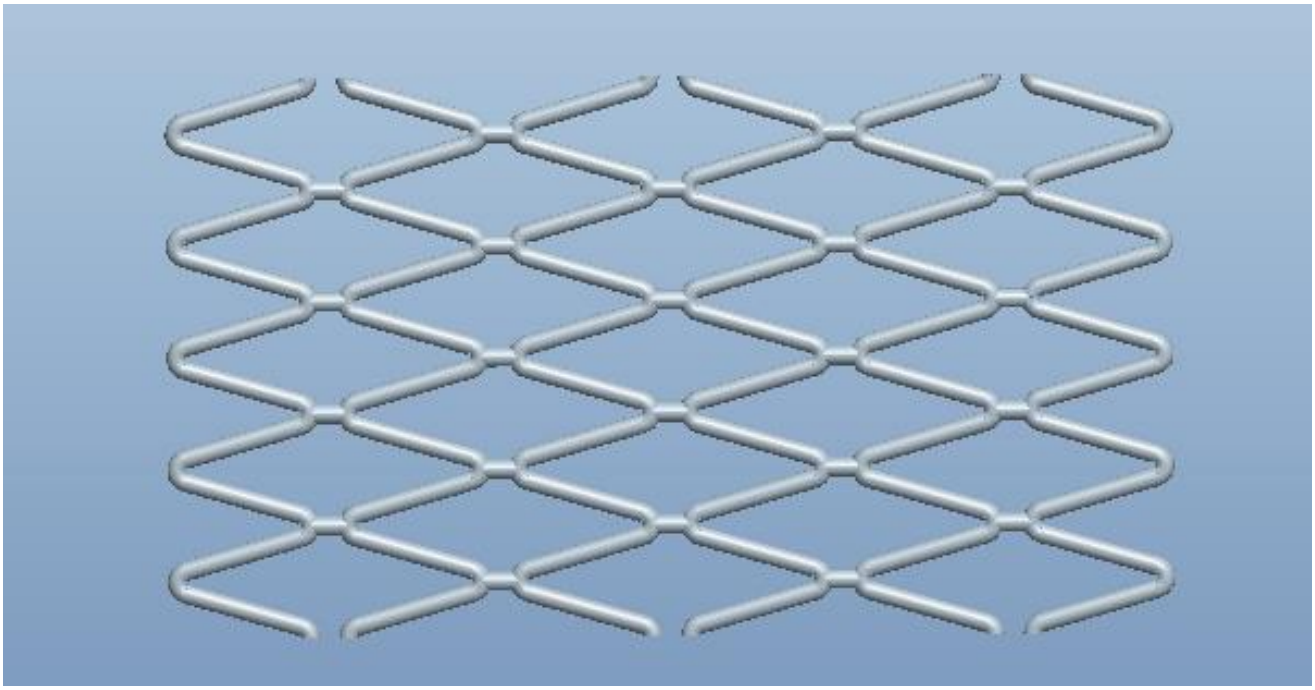

Figure 24 3D flat surface of biodegradable stents by sweep feature

Finally, the function of Toroidal Bend (Figure 24) is used to shape the flat surface into the tube. The Toroidal Bend command can bend solids, surfaces or datum curves into shapes. This command gets accustomed to creating tire-like structures, where the customers need to create operations on a flat surface and then bend it.

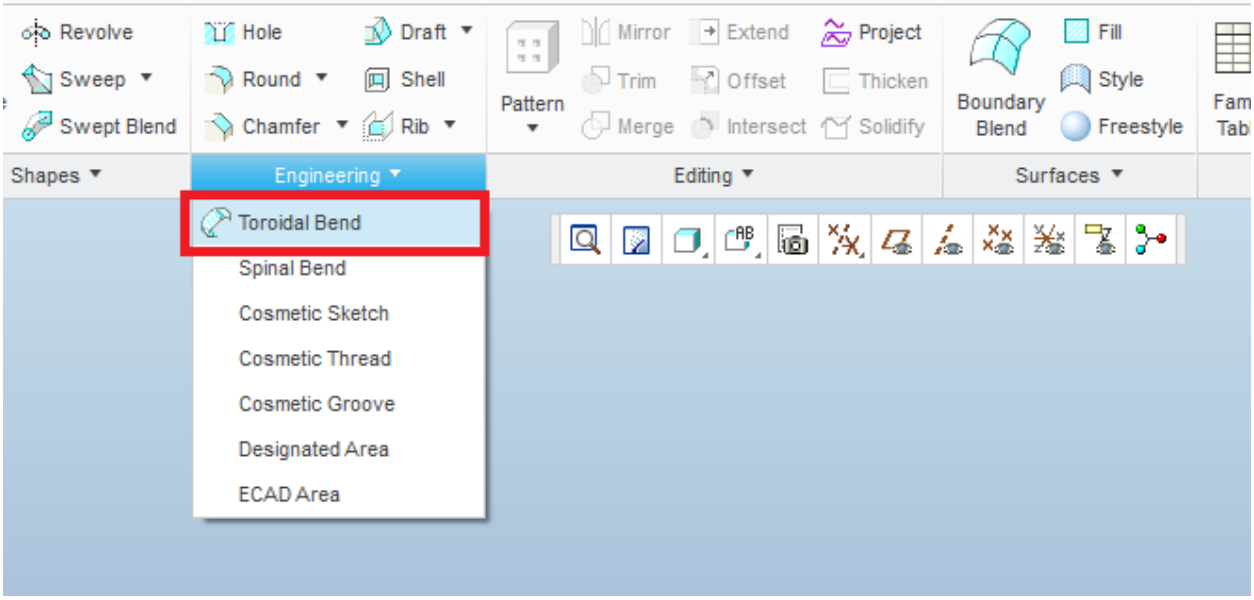

Figure 25 Toroidal Bend feature in Pro/Engineer

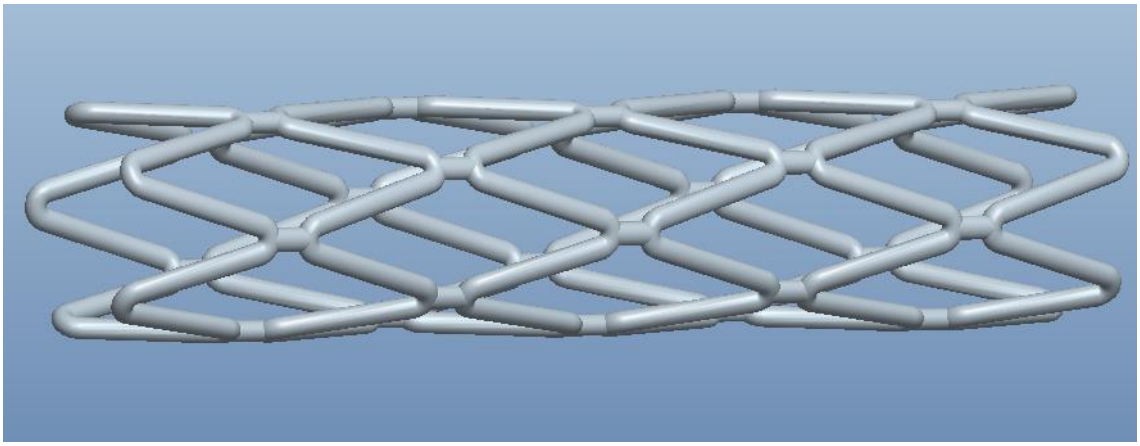

Figure 26 Model of biodegradable stents built in Pro/Engineer

Through the main three features, a 3D parametric model of the zigzag stent has been created (Figure 25). In the next section, the 3D parametric model will be used to simulate the compression test, which has been carried out in chapter 4.

5.3 Simulation of Compression Test with the Finite Element Analysis Method

The simulation of compression test of biodegradable stents will be performed by a static structural analysis that can determine the displacements, stresses, strains, and forces in structures or components caused by loads that do not induce significant inertia and damping effects [54]. Steady loading and response conditions are assumed; that is, the loads and the structure's response are assumed to vary slowly with respect to time. The results of the simulation will show the load-displacement curve for the biodegradable stents.

For a linear static structural analysis, the displacements {x} are solved in the matrix equation below [55]:

$$[K]\{x\} = \{F\} \tag{5.1}$$

This results in certain assumptions related to the analysis:

- [K] is essentially constant. The linear elastic material behavior is assumed, and small deflection theory is used.

- {F} is statically applied. No time-varying forces are considered, and no inertial effects (mass, damping) are included.

5.3.1 Procedure of Finite element simulation

1. *Project Schematic*

The innovative project schematic view can transform the way engineers work with the simulation. Projects are represented graphically as connected systems in a flowchart-like diagram. There are many systems for specific analysis in Toolbox, and each system in the Toolbox can be dropped into the Project Schematic window as shown in Figure 26. The system of Static Structural analysis is selected and dropped; then, the Geometry can be linked and shared.

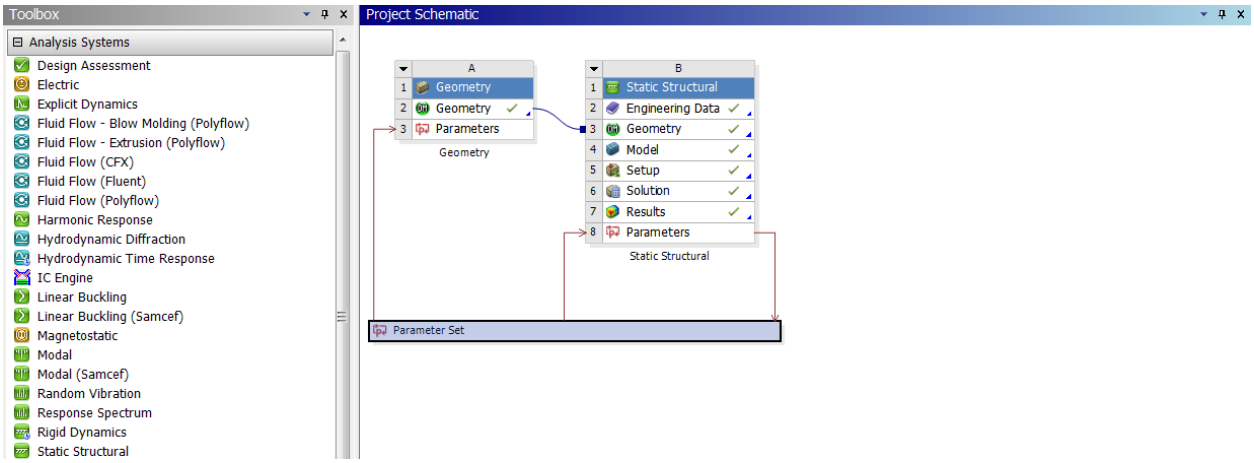

Figure 27 Project schematic view

2. *Geometry Import*

It is more efficient to import the CAD model into ANSYS than to re-create it if the geometry of the part has been created. There are various import options available in ANSYS, such as IGES Imports and Connection Products. IGES importing works quite easily, but because of the dual translation process- CAD – IGES- ANSYS, in many cases where it does not function well. While ANSYS Connection products overcome this problem by directly reading the "native" part files produced by the CAD package like connection for Pro/Engineer (Figure 27). The geometry of biodegradable stents is imported directly from Pro/Engineer to ANSYS in this simulation process (Figure 28).

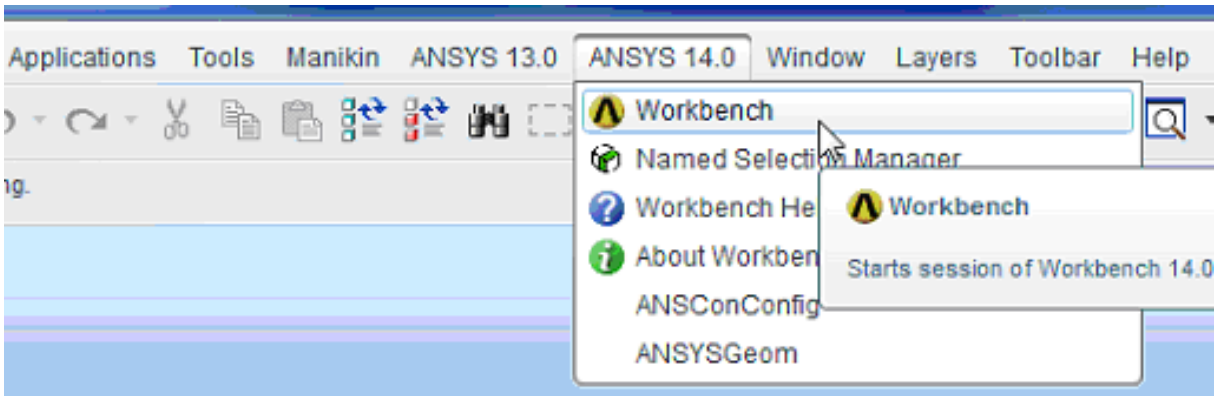

Figure 28 Geometry import process

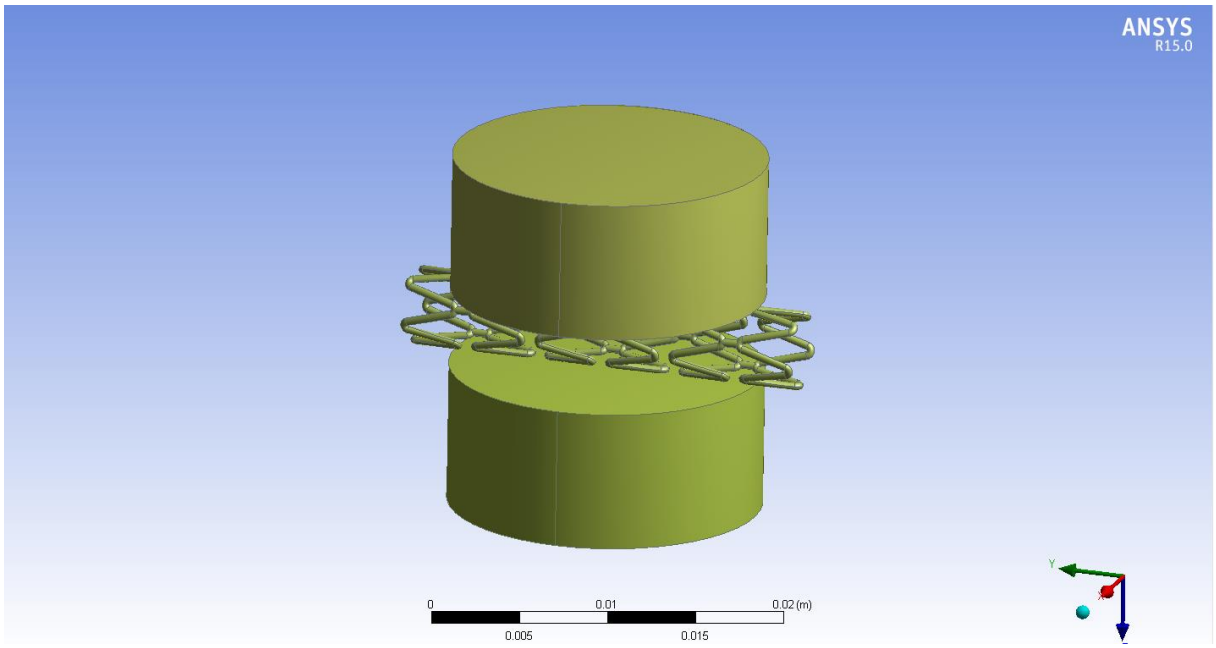

Figure 29 Geometry of model

3. *Material properties*

The Engineering Data Manager in ANSYS Workbench provides a powerful tool for defining, organizing, and storing material properties. A great variety of material models are available in the Toolbox menu, and material data can be stored in libraries that can be accessed in any project. The biodegradable stent is made of PCL while the compression plates are made of structural steel. The material properties [56] defined are density, Young's Modulus and Poisson's Ratio (Fig. 29-31).

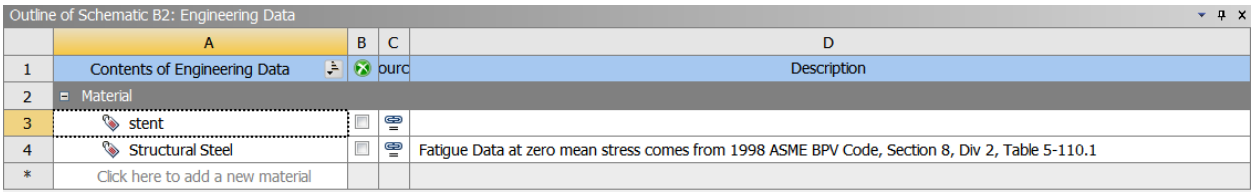

Outline of Schematic B2: Engineering Data

	A	B	C	D
1	Contents of Engineering Data		ourc	Description
2	Material			
3	stent			
4	Structural Steel			Fatigue Data at zero mean stress comes from 1998 ASME BPV Code, Section 8, Div 2, Table 5-110.1
*	Click here to add a new material			

Figure 30 Engineering data manager

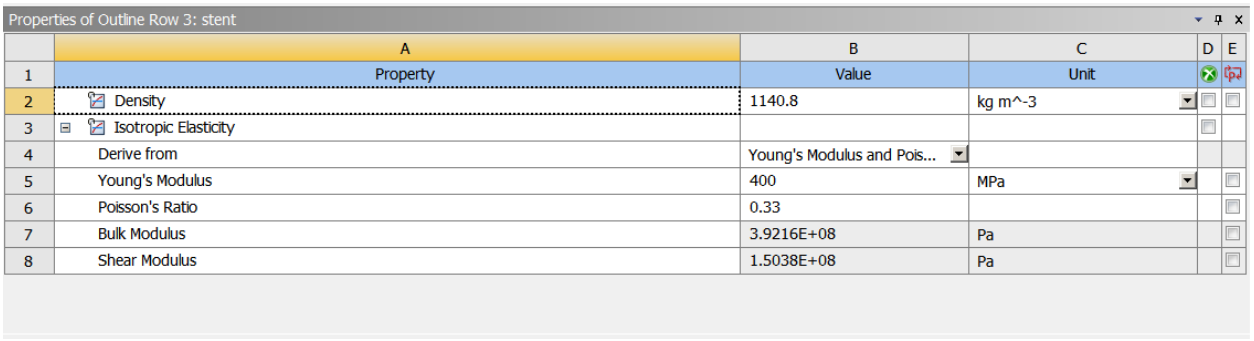

Properties of Outline Row 3: stent

	A	B	C	D	E
1	Property	Value	Unit		
2	Density	1140.8	kg m^-3		
3	Isotropic Elasticity				
4	Derive from	Young's Modulus and Pois...			
5	Young's Modulus	400	MPa		
6	Poisson's Ratio	0.33			
7	Bulk Modulus	3.9216E+08	Pa		
8	Shear Modulus	1.5038E+08	Pa		

Figure 31 Properties of PCL (material of biodegradable stent)

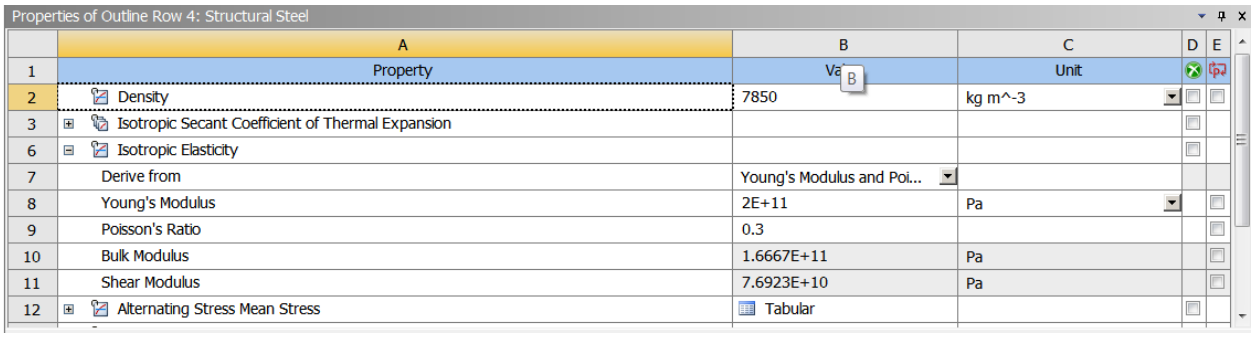

Properties of Outline Row 4: Structural Steel

	A	B	C	D	E
1	Property	Va	Unit		
2	Density	7850	kg m^-3		
3	Isotropic Secant Coefficient of Thermal Expansion				
6	Isotropic Elasticity				
7	Derive from	Young's Modulus and Poi...			
8	Young's Modulus	2E+11	Pa		
9	Poisson's Ratio	0.3			
10	Bulk Modulus	1.6667E+11	Pa		
11	Shear Modulus	7.6923E+10	Pa		
12	Alternating Stress Mean Stress	Tabular			

Figure 32 Properties of Structural Steel (material of compression plates)

4. *Meshing*

Meshing is an essential part of the computer-aided engineering simulation process. The mesh influences the accuracy, convergence and the speed of the solution. Furthermore, the time that it takes to create and mesh a model plays a significant role in the time it takes to get results from a CAE solution. Therefore, the better and more automated the meshing tools, the better the solution. The Mesh Tool in ANSYS Workbench provides an accessible path to many of the most common mesh controls. The Tetrahedral meshing method is used for meshing biodegradable stents. This method uses a bottom-up approach (creates a surface mesh then volume mesh), and multiple triangular surface meshing algorithms are applied to ensure a high quality (Figure 32) [57]. The surface mesh is generated first, and then from the surface mesh, inflation layers can be grown. There are 99249 nodes and 43712 elements totally in Figure 33.

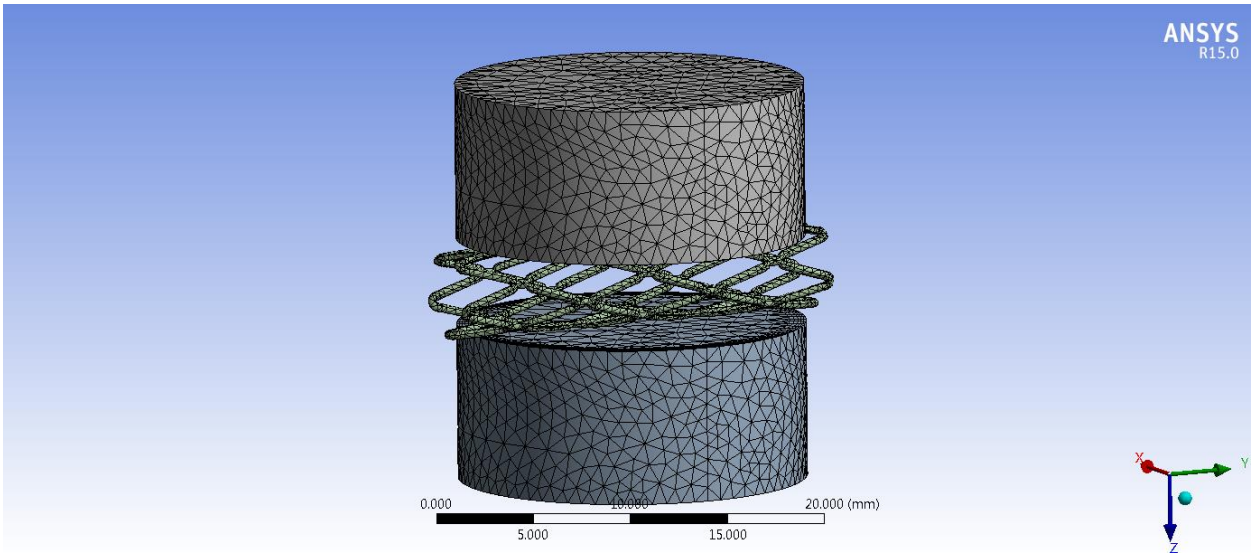

Figure 33 Meshed biodegradable stents with plates

Statistics	
Nodes	99249
Elements	43712

Figure 34 Numbers of nodes and elements

5. *Boundary Conditions*

Based on the equipment in the real compression test, the upper plate is fixed, and the plate below can be moved with the force applied. Therefore, the fixed support is used on the top plate (Figure 34), and the displacement of X and Y direction on the lower plate is zero while the displacement of z-direction is free. Additionally (Figure 35), the initial force is - 0.2 N with the opposite Z direction (Figure 36).

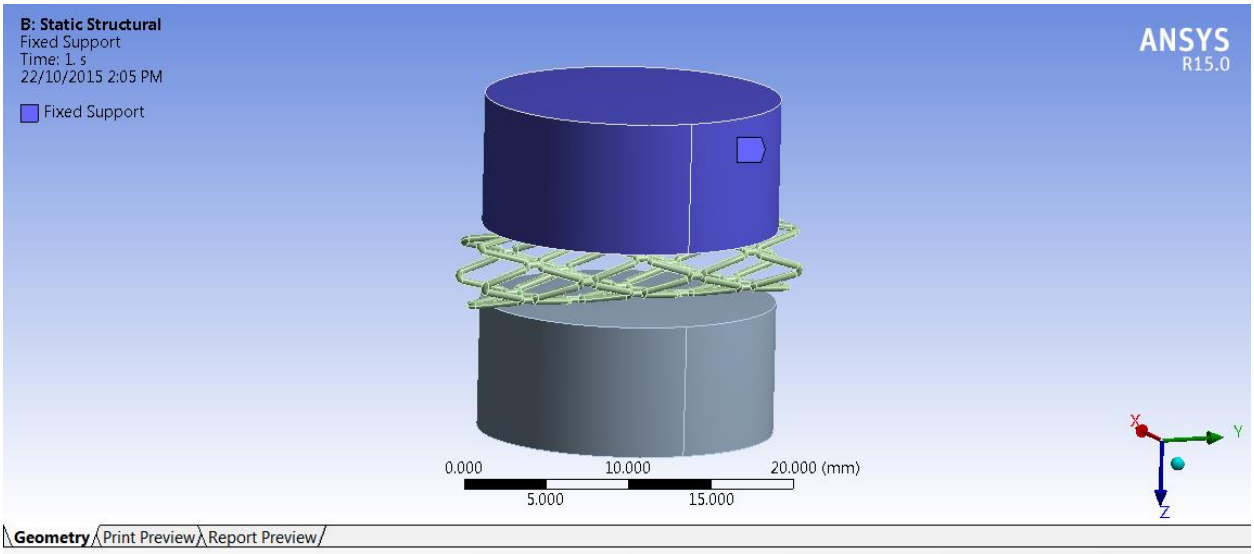

Figure 35 Fixed support on the upper plate

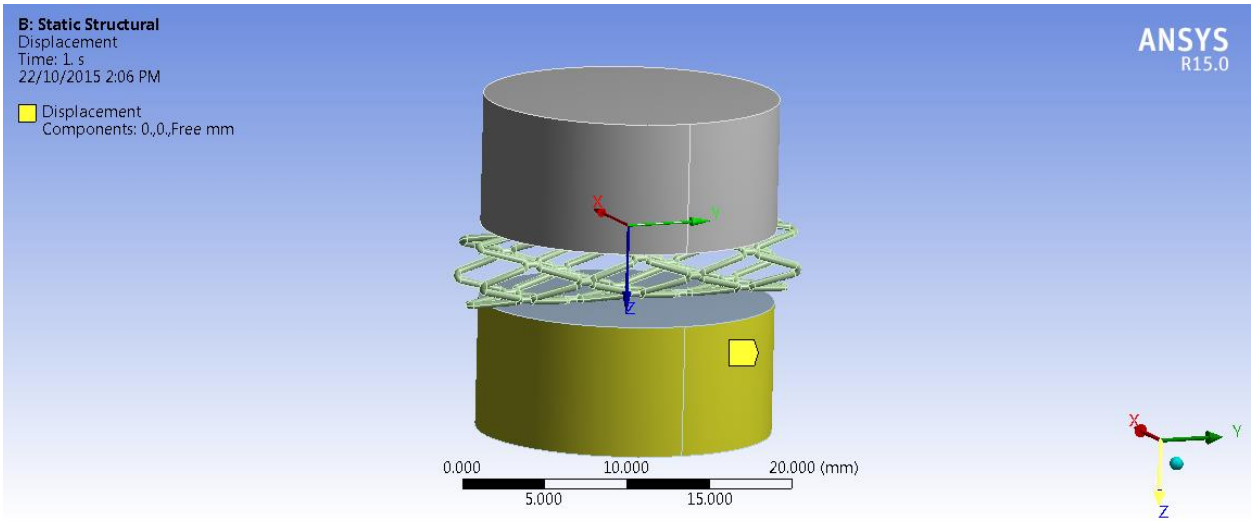

Figure 36 Displacement setting on the lower plate

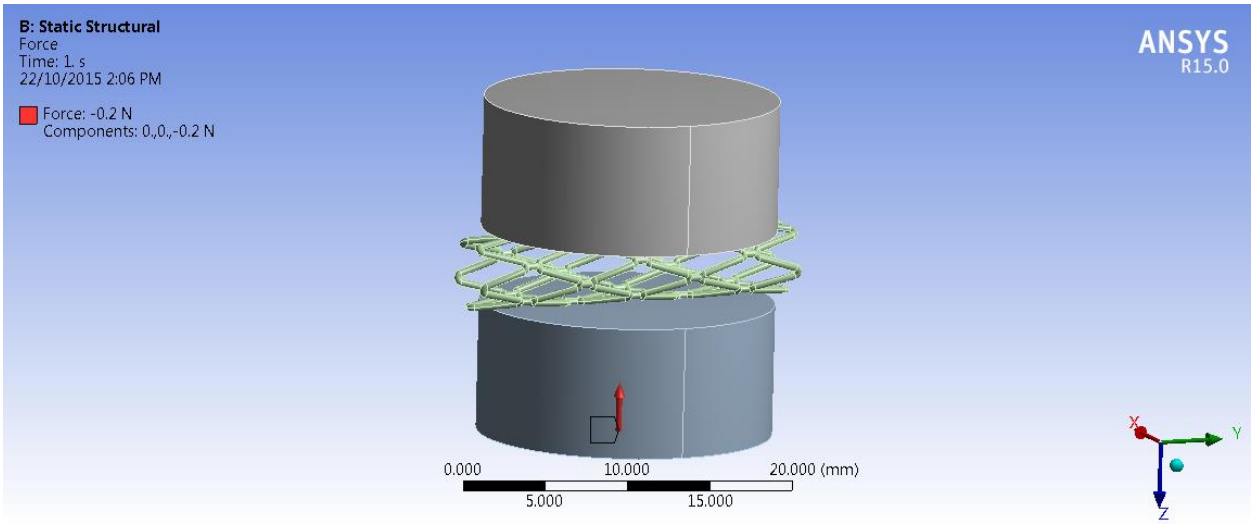

Figure 37 Force applied on the lower plate

5.3.2 Results

The results present the total deformation of biodegradable stents. According to the real compression test, the forces required to compress biodegradable stents radially 10% (0.342mm) is 0.199 N. When the force is 0.199 N applied in the simulation, the total deformation of the biodegradable stent is 0.304 mm (Figure 37), the error is 11.11%. Then the force compressing biodegradable stents radially 20% is applied on the biodegradable stent in the simulation, and the total deformation of the biodegradable stent are 0.681 mm, and the error is 0.29% compared with the real compression test (0.679 mm in Figure 38).

The deformation comparison of biodegradable stents between simulation and actual compression test shows in Table 6 and the curve comparison is presented in Figure 39. The relationship between force and deformation is linear in the simulation of ANSYS Workbench while in the actual compression test the relationship between force and deformation is non-linear. The error based on the comparison results (the maximum error 13.14%) is insignificant, indicating that the finite element model is acceptable within the range of around 20% radial deformation.

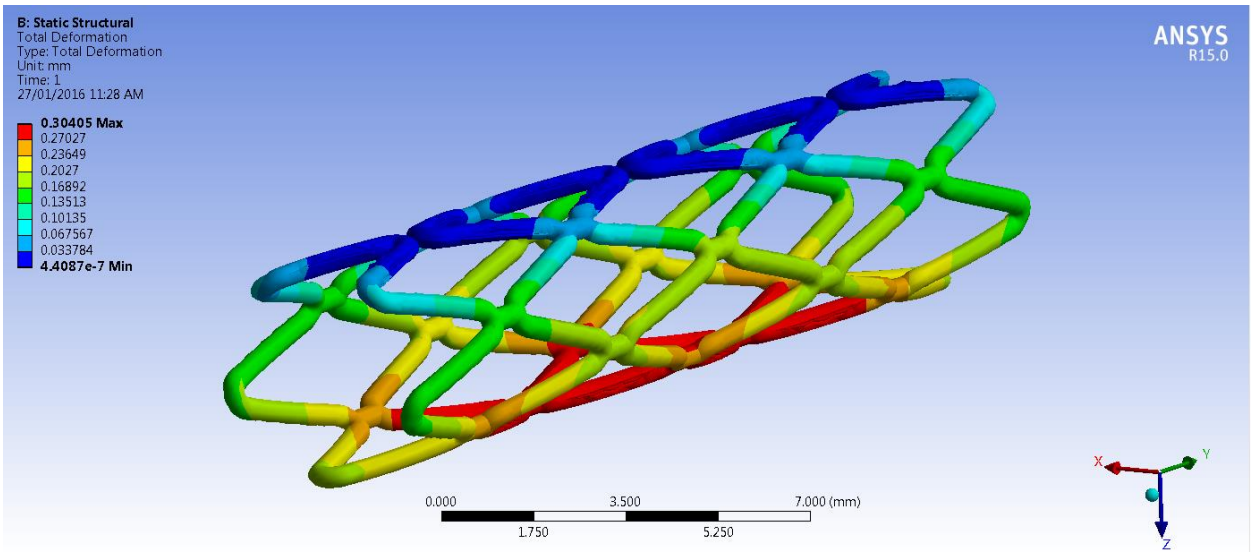

Figure 38 Deformation of compressing biodegradable stents radially 10%

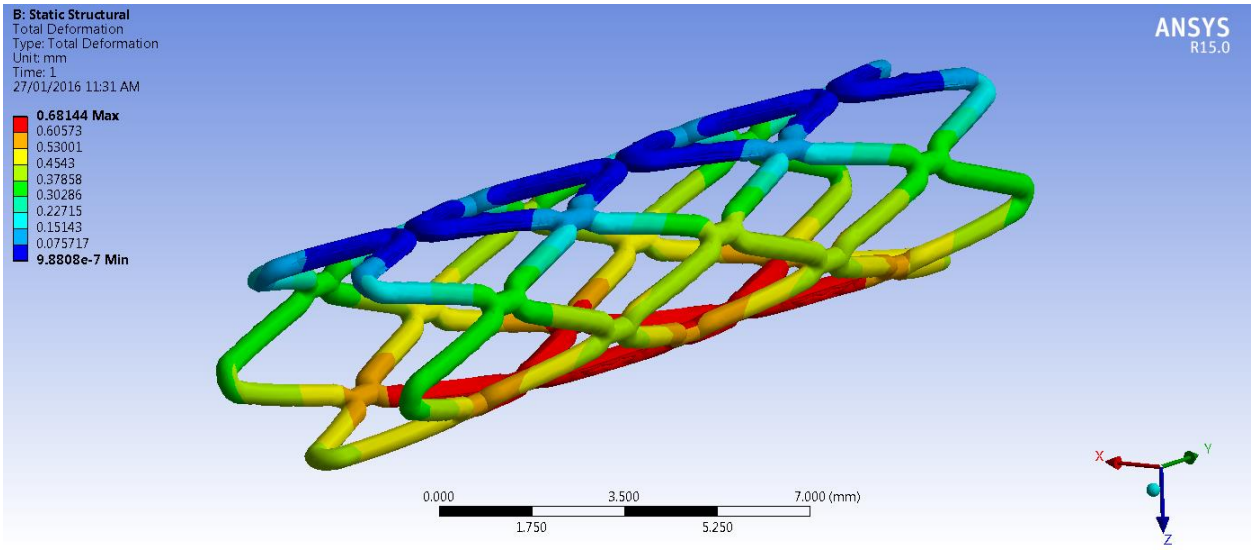

Figure 39 Deformation of compressing biodegradable stents radially 20%

Table 6 Deformation comparison between simulation of biodegradable stents and real compression test

Force (N)	Maximum Total Deformation in Simulation (mm)	Deformation in Compression Test (mm)	Errors
0.026	0.040	0.036	11.11%
0.049	0.075	0.069	8.70%
0.072	0.110	0.101	8.91%
0.085	0.130	0.136	-4.41%
0.107	0.163	0.174	-6.32%
0.120	0.183	0.206	-11.17%
0.139	0.212	0.238	-10.92%
0.156	0.238	0.274	-13.14%
0.176	0.269	0.306	-12.09%
0.199	0.304	0.342	-11.11%
0.222	0.339	0.376	-9.84%
0.249	0.380	0.406	-6.40%
0.271	0.414	0.444	-6.76%
0.295	0.451	0.475	-5.05%
0.332	0.507	0.513	-1.17%
0.354	0.541	0.544	-0.55%
0.375	0.573	0.576	-0.52%
0.406	0.620	0.616	0.65%
0.425	0.649	0.644	0.78%
0.446	0.681	0.679	0.29%

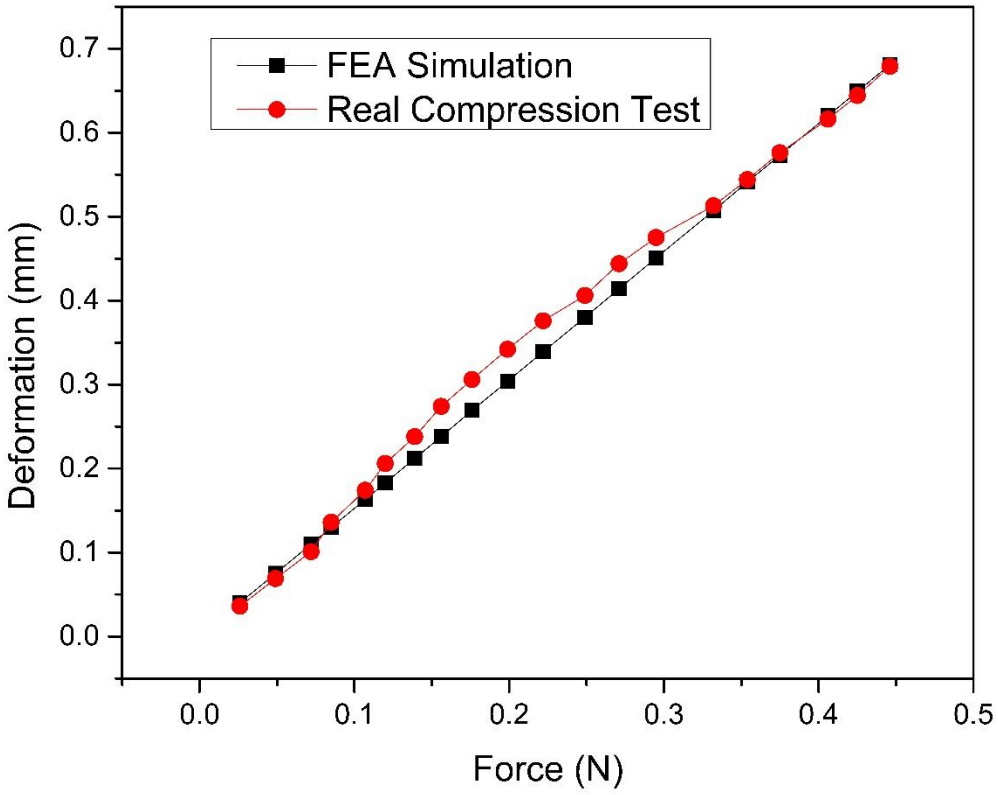

Figure 40 Total deformation and force relationship comparison between FEA and real compression test

5.4 Conclusions

The deformation comparison of biodegradable stents between simulation and actual compression test shows that the finite element model for simulating the compression test can be accepted within the range of around 20% radial deformation. The simulation model of biodegradable stent is to be used for optimization of stents, as presented in the next chapter to improve the radial stiffness.

CHAPTER 6 Optimal-Design of Biodegradable Stents and Simulation of Biodegradable Stents in the Blood Vessel

6.1 Introduction to Optimization Methods in ANSYS Workbench

A brief introduction to parametric optimization based on Static Structure simulations is presented. ANSYS DesignXplorer is a design optimization application that works under the ANSYS Workbench environment [60]. ANSYS DesignXplorer interacts with all ANSYS Workbench platform components and leads CAD packages directly such as Pro/ENGINEER so that design changes can be quickly made to the design database [60]. Therefore, the simulation model of biodegradable stents built in chapter 5 can be used for parametric optimization. The instantaneous feedback on design modifications provided by ANSYS DesignXplorer dramatically decreases the number of design iterations.

The DesignXplorer's systems (parameters correlation, direct optimization, response surface, and response surface optimization or Six Sigma analysis) to the Workbench schematic are with drag-and-drop simplicity (Figures 40 and 41). Response surface systems are equipped with a variety of design of experiment (DOE) algorithms to efficiently and scientifically sample the design space. The main idea of response surface methodology is to use a sequence of designed experiments to obtain an optimal response. The resulting approximation of the output parameter as a function of the input variables is called the response surface. Single- and multi-objective optimization algorithms can use the multi-dimensional response surface to find the optimal design quickly. Advanced direct optimization is also useful, along with adaptive optimization algorithms that combine the best function of response-surface and direct optimization [61].

Figure 41 DesignXplorer's systems

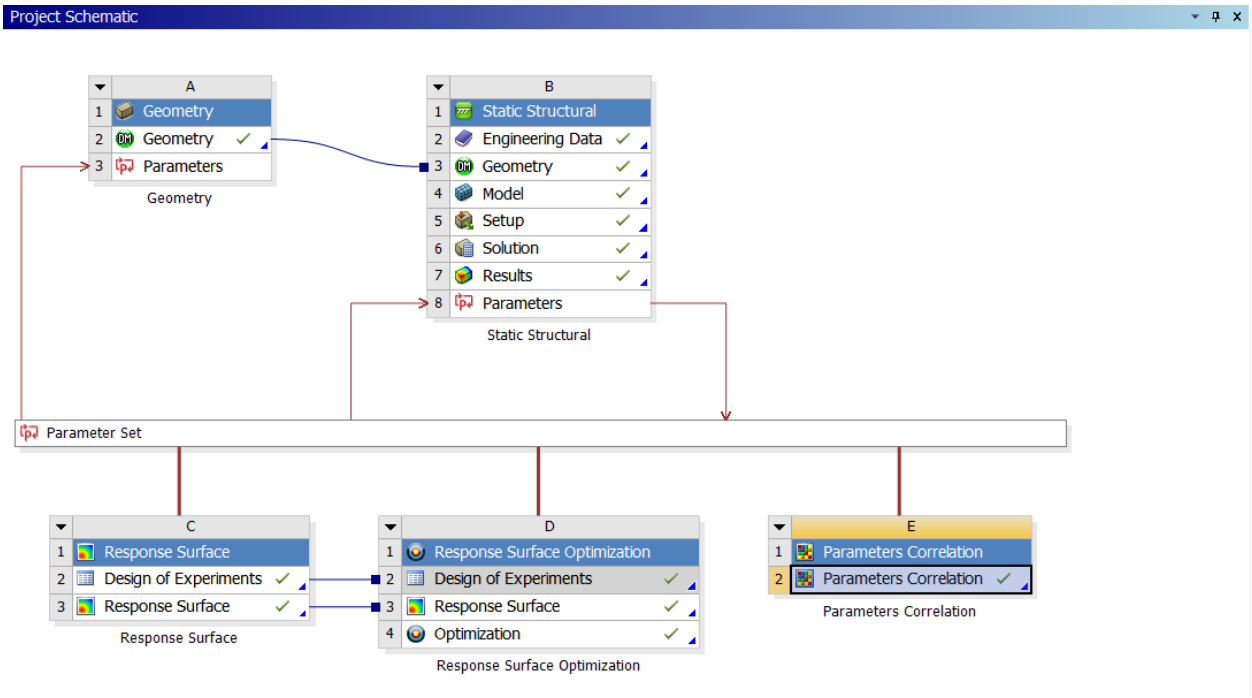

Figure 42 Project Schematic of parametric optimization of biodegradable stents

The goal here is to determine the parameters of the biodegradable stent that offer the minimum radial deformations under the given force. With the design of experiments, several combinations of the parameters are created as "design points". By running the analysis for each design point and recording the output, a mathematical formula was fitted to the data, which is called a "response surface." The parameters are determined from this formula with a significant effect on the outputs.

6.2 Optimization of the Biodegradable stents with DesignXplorer

6.2.1 Design of Experiment

In the project setup, design optimization requires identification of input and output parameters. The input parameters are geometric parameters （A, B and C）defined in Chapter 5 (Figures 42 and 43). The output parameter is the deformation of the biodegradable stent. Each combination of input parameters used is called a design point. The design of experiments specifies changes in input parameters to observe the corresponding output response (Figure 44).

Outline of Schematic C2: Design of Experiments

	A	B
1		Enabled
2	Design of Experiments	
3	Input Parameters	
4	Geometry (A1)	
5	P1 - DS_A	☑
6	P2 - DS_B	☑
7	P3 - DS_C	☑
8	Output Parameters	
9	Static Structural (B1)	
10	P4 - Total Deformation Maximum	
11	Charts	
12	Parameters Parallel	
13	Design Points vs Parameter	

Figure 43 Input and output parameters in design of experiments

Properties of Outline A5: P1 - DS_A

	A	B
1	Property	Value
2	General	
3	Units	
4	Type	Design Variable
5	Classification	Continuous
6	Values	
7	Value	0.25
8	Lower Bound	0.21
9	Upper Bound	0.3
10	Use Manufacturable Values	

(a) Parameter A

Properties of Outline A6: P2 - DS_B

	A	B
1	Property	Value
2	General	
3	Units	
4	Type	Design Variable
5	Classification	Continuous
6	Values	
7	Value	2.8
8	Lower Bound	2.4
9	Upper Bound	3.2
10	Use Manufacturable Values	

(b) Parameter B

Properties of Outline A7: P3 - DS_C

	A	B
1	Property	Value
2	General	
3	Units	
4	Type	Design Variable
5	Classification	Continuous
6	Values	
7	Value	0.8
8	Lower Bound	0.6
9	Upper Bound	1
10	Use Manufacturable Values	

(c) Parameter C

Figure 44 Values setting for input parameters

Properties of Outline A2: Design of Experiment

	A	B
1	Property	Value
2	Design Points	
3	Preserve Design Points After DX Run	
4	Failed Design Points Management	
5	Number of Retries	0
6	Design of Experiments	
7	Design of Experiments Type	Central Composite D...
8	Design Type	Auto Defined

Figure 45 Design of experiments type

6.2.2 Response Surface and sensitivity

In statistics, response surface methodology explores the relationships between several explanatory variables and one or more response variables. The major idea of response surface

method is to use a sequence of designed experiments to obtain an optimal response (Figure 45). A second-degree polynomial model is suggested for use because such a model is easy to establish and apply (Figure 46). Once the relationship is determined, the resulting approximation of the output parameter as a function of the input variables is called the response surface.

Outline of Schematic C3: Response Surface

	A	B
1		Enabled
2	Response Surface	
3	Input Parameters	
4	Geometry (A1)	
5	P1 - DS_A	☑
6	P2 - DS_B	☑
7	P3 - DS_C	☑
8	Output Parameters	
9	Static Structural (B1)	
10	P4 - Total Deformation Maximum	
11	Min-Max Search	☑
12	Metrics	
13	Goodness Of Fit	
14	Response Points	
15	Response Point	
16	Response	

Figure 46 Input and output parameters in response surface

Properties of Schematic C3: Response Surface

	A	B
1	Property	Value
2	Design Points	
3	Preserve Design Points After DX Run	☐
4	Failed Design Points Management	
5	Number of Retries	0
6	Meta Model	
7	Response Surface Type	Standard Response Surface - Full 2nd Ord...
8	Refinement	
9	Refinement Type	Manual
10	Verification Points	
11	Generate Verification Points	☐

Figure 47 Response surface type

The response surface charts show the relationship between parameters (A, B, and C) and total deformation in Figures 47- 49. As defined in Chapter 5, A is the diameter of curvature at the apex. As the diameter of curvature changes, the angle between two lines will be altered. B is the vertical length of the line tangential with the semi-circle. C is the distance between two apexes of

the semi-circles. In Figure 47, the total deformation has little changed with the parameter A at range from 0.21 mm to 0.3 mm. The line in Figure 48 grows quickly, which means that parameter B plays a significant role in total deformation of biodegradable stents. When parameter B is 2.4 mm, the total deformation is approximately 0.38mm. While the total deformation is about 0.78 mm when parameter B is 3.2 mm. The result shows that the better total deformation can be obtained by reducing the length of the line tangential with the semi-circle. Figure 49 shows that the minimum total deformation can be obtained when parameter C is around 0.8 mm. Apparently, the larger distance between two apexes of the semi-circles causes more deformation of the biodegradable stents.

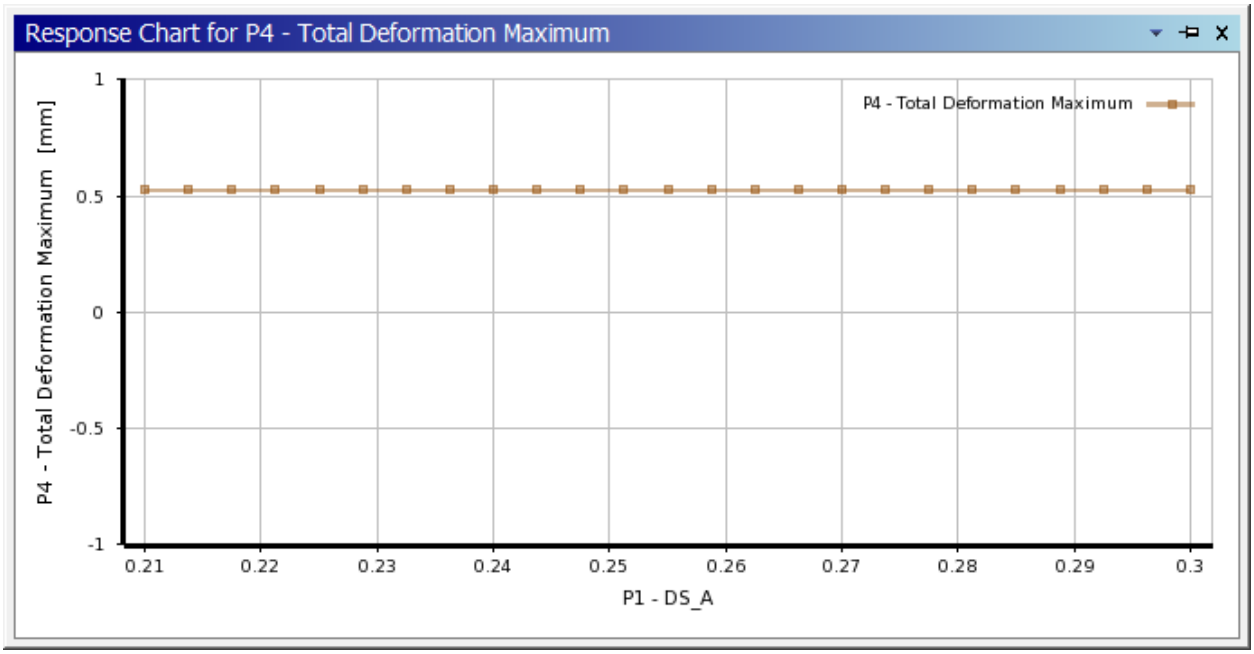

Figure 48 2D Response chart for total deformation and parameter A

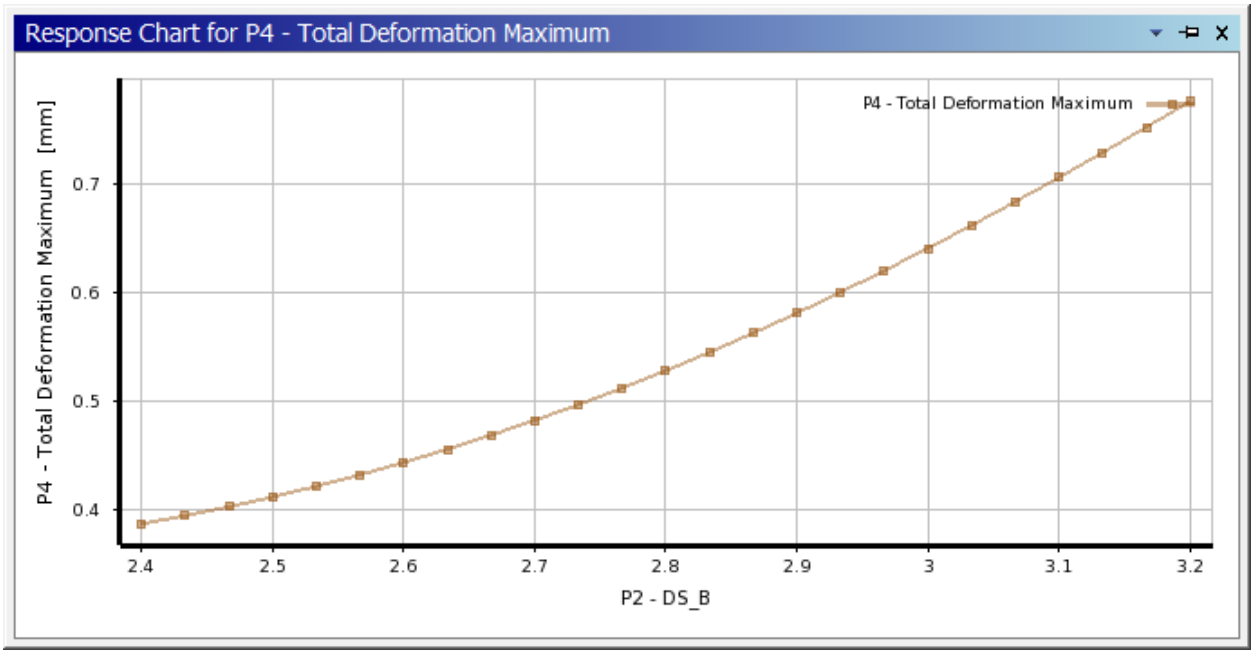

Figure 49 2D Response chart for total deformation and parameter B

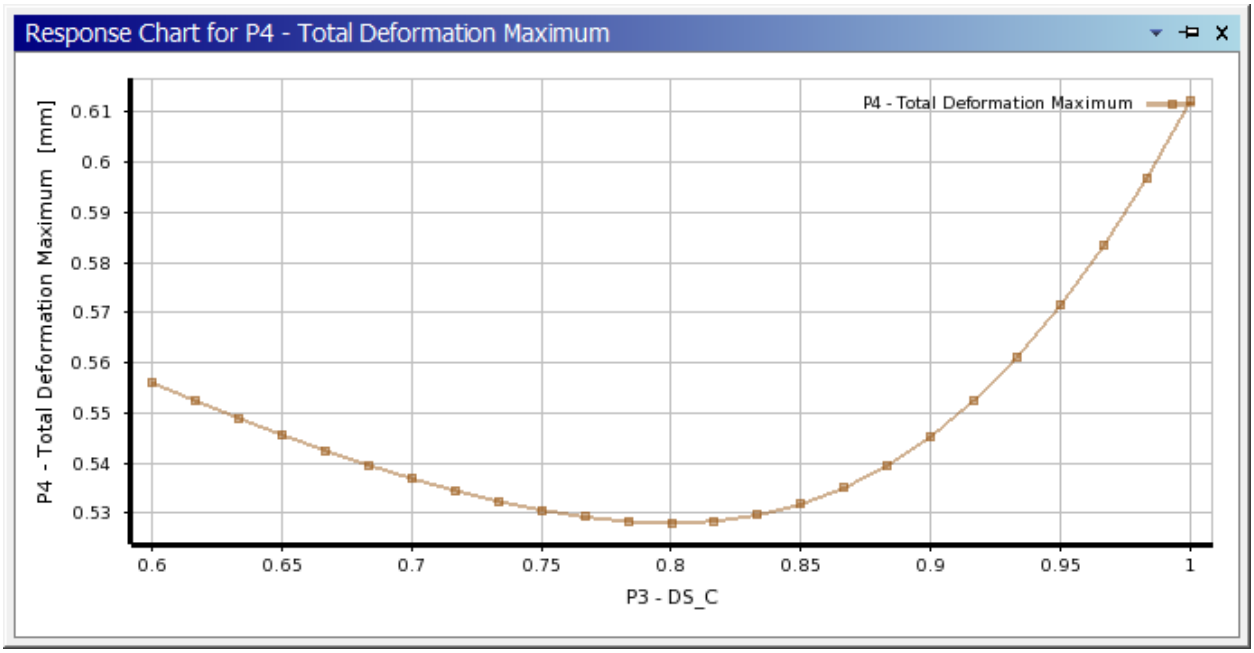

Figure 50 2D Response chart for total deformation and parameter C

The charts below are the 3D response charts for total deformation and parameters. Axes of X and Y represent the different parameters while Z-axis represents the total deformation of biodegradable stents. From Figure 50, it can be seen that the total deformation increases with the growth of parameter B, as parameter A has little effect on the total deformation. In Figure 51, the

trend of the total parameter is the same as the 2D response chart (Figure 49), as the parameter C plays greater role than parameter A. Figure 52 shows that the total deformation of biodegradable stents is influenced by both parameter B and C.

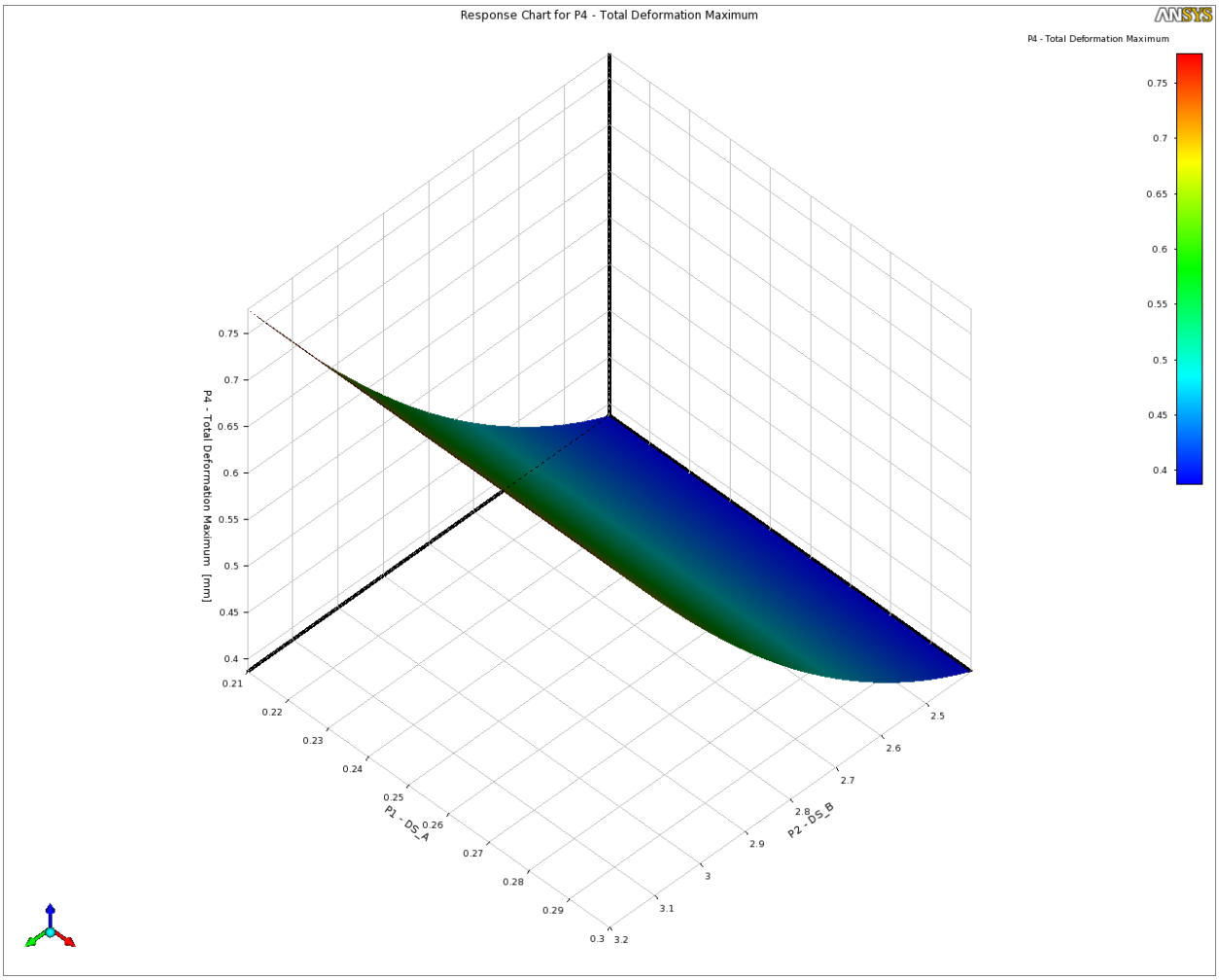

Figure 51 3D Response chart for total deformation, parameter A and parameter B

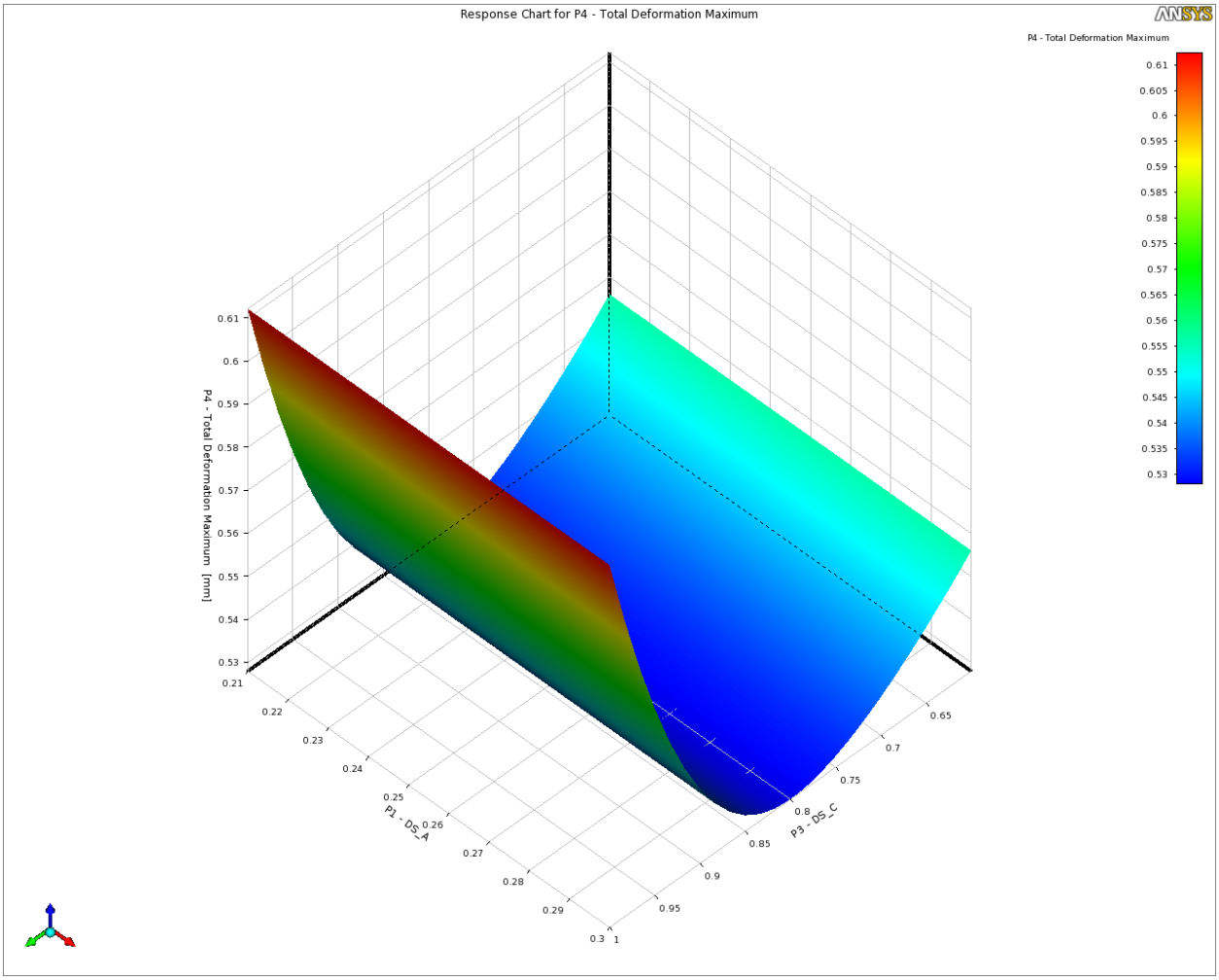

Figure 52 3D Response chart for total deformation, parameter A and parameter C

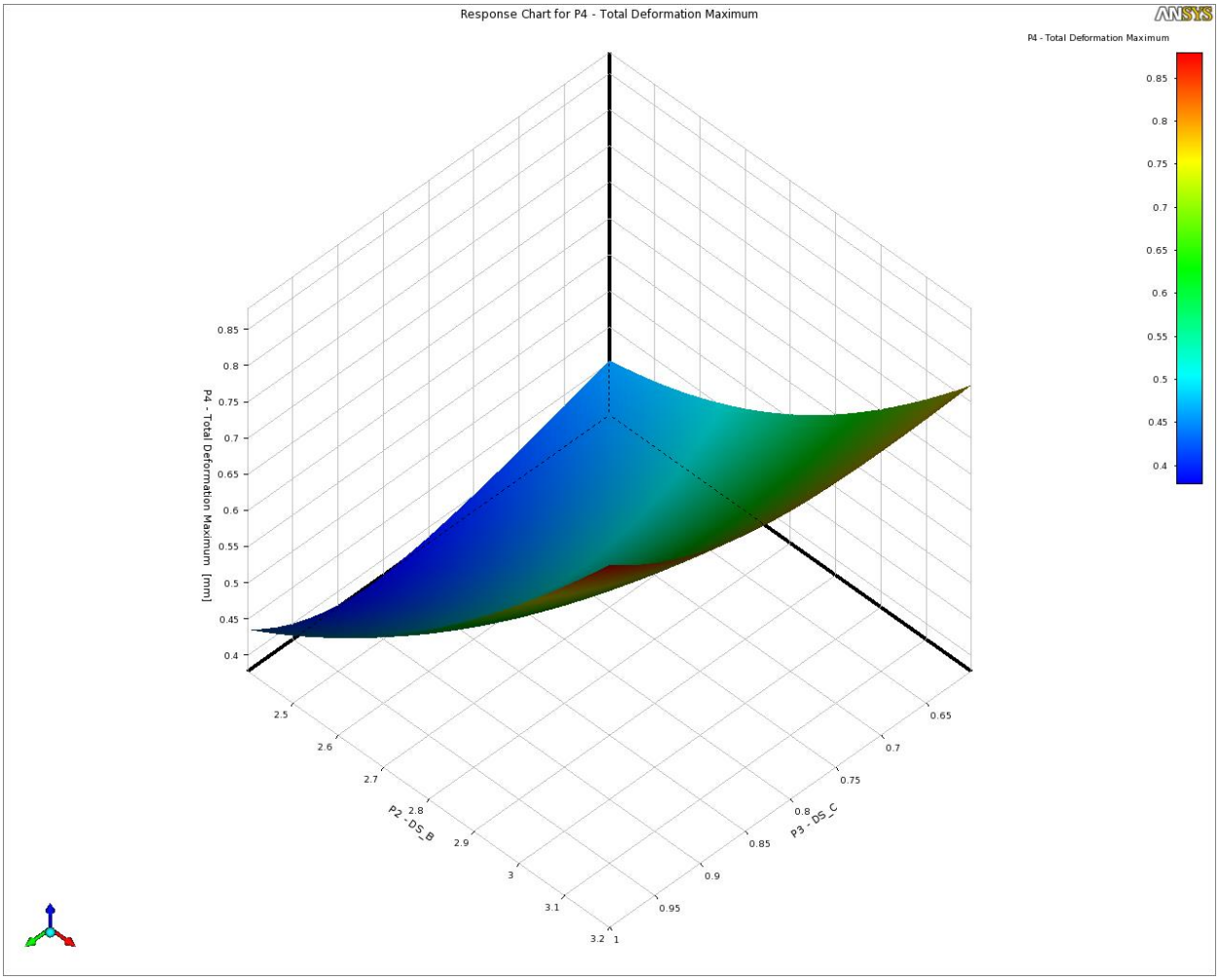

Figure 53 3D Response chart for total deformation, parameter B, and parameter C

6.2.3 Sensitivity Analysis

The sensitivity can be a powerful exploration tool to represent the impact of the input parameters on the output parameters. The resulting chart provides the weight of the different inputs for the output. In the Fig. 53, it shows that Parameter B has a significant effect on the total deformation, while Parameter A has little influence on the total deformation. Parameter C displays the medium impact on the total deformation of biodegradable stents.

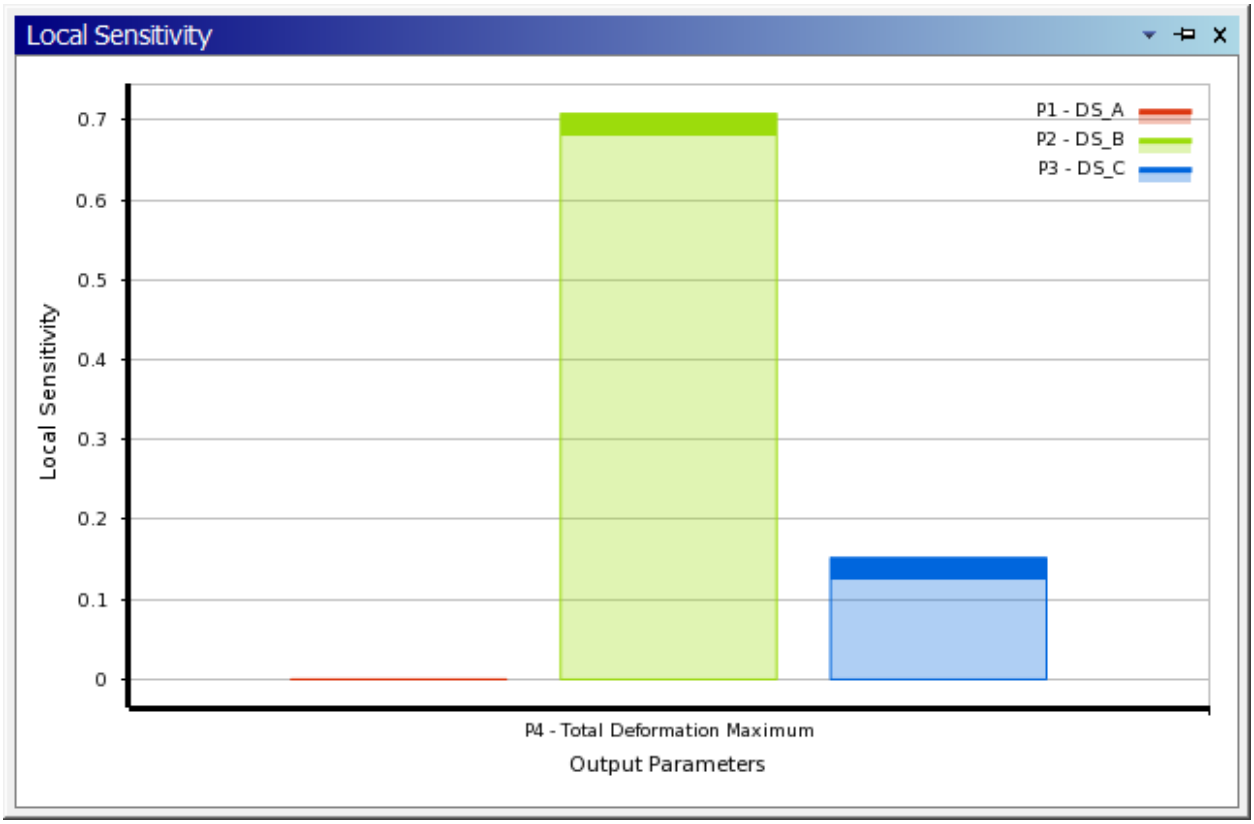

Figure 54 Sensitivity Analysis

6.2.4 Optimization process and results

In the optimization properties, one or more objectives with or without constrains can be set (Figure 54). The direct optimization component in ANSYS Workbench offers several methods for single and multi-objective optimization such as Screening, Multi-objective generic algorithm and Nonlinear Programming by quadratic Lagrangian. In this project, the screening method is used, which is a simple approach based on sampling and sorting. A screening method is a direct method that creates a sample set of the design points and sorts them based on the objectives. It is a powerful way of obtaining the approximate vicinity of global minima and is proper for use in preliminary design [55]. There are 10000 samples to sort for the objective shown in Figure 55.

Outline of Schematic D4: Optimization

	A	B	C
1		Enabled	Monitoring
2	Optimization		
3	Objectives and Constraints		
4	Minimize P4		
5	Domain		
6	Geometry (A1)		
7	P1 - DS_A	☑	
8	P2 - DS_B	☑	
9	P3 - DS_C	☑	
10	Parameter Relationships		
11	Results		
12	Candidate Points		
13	Tradeoff		
14	Samples		
15	Sensitivities		

Figure 55 Outline of schematic for optimization

Properties of Outline A2: Method

	A	B
1	Property	Value
2	Design Points	
3	Preserve Design Points After DX Run	☐
4	Failed Design Points Management	
5	Number of Retries	0
6	Optimization	
7	Method Name	Screening
8	Verify Candidate Points	☐
9	Number of Samples	10000
10	Maximum Number of Candidates	3
11	Optimization Status	
12	Converged	Yes
13	Number of Evaluations	10000
14	Number of Failures	0
15	Size of Generated Sample Set	10002
16	Number of Candidates	3

Figure 56 Optimization method settings

Table of Schematic D4: Optimization , Candidate Points

	A	B	C	D	E	F	G
1	Reference	Name	P1 - DS_A	P2 - DS_B	P3 - DS_C	P4 - Total Deformation Maximum (mm)	
2						Parameter Value	Variation from Reference
3	◉	Candidate Point 1	0.24749	2.4	0.86518	★★★ 0.3783	0.00 %
4	○	Candidate Point 2	0.26765	2.4043	0.77578	★★★ 0.39385	4.11 %
5	○	Candidate Point 3	0.25325	2.4238	0.68799	★★ 0.42499	12.34 %
*		*New Custom Candidate Point*	*0.255*	*2.8*	*0.8*		

Figure 57 Candidate designs

The optimization results are now shown with ratings (the more stars, the better). Candidate point 1 is in this case the best choice, among the 10000 sampled points, and the total deformation of biodegradable stents will be 0.3783 mm (Figure 56). Compared with the initial total deformation (0.5887 mm) when applying the force (-0.4N) to compress the biodegradable stent, it decreases by 35%, which makes a significant contribution to increasing the mechanical property. The parameters obtained from the optimization are 0.247 mm for A, 2.4 mm for B and 0.865 mm for C.

6.3 FEA simulation of Biodegradable Stent in the Blood Vessel

The total deformation of the optimized model of the biodegradable stent in a blood vessel is expected to investigate through a simulation of static analysis. The procedure consists of modeling geometry, setting material properties, applying boundary conditions and loads and viewing results.

6.3.1 Modelling geometry

The geometry consists of two parts: blood vessel and stent (Figures 57 and 58). Firstly, the CAD models are built in the Pro/Engineering Software. The length of the blood vessel is 29 mm, the inner diameter of the blood vessel is 3.4 mm, and the thickness of artery is 0.5 mm [59]. The length of the biodegradable stent is 23 mm, the outer diameter of the stent is 3.4 mm, and the diameter of the struts is 0.41 mm.

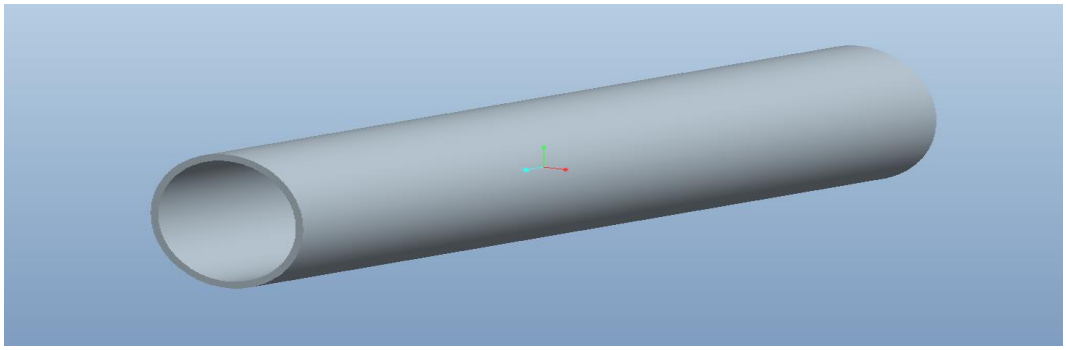

Figure 58 CAD model of blood vessel

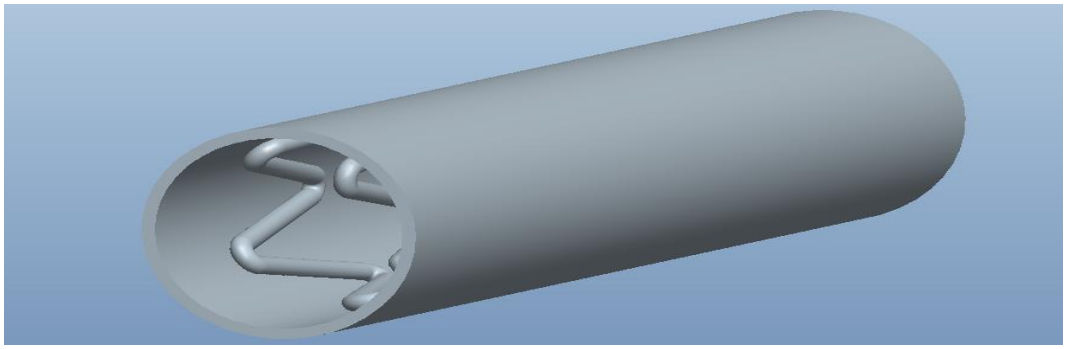

Figure 59 CAD model of a biodegradable stent with blood vessel

Then, the CAD model can be imported into ANSYS Workbench through the connection package that is the same import method used in the last section (Figure 59).

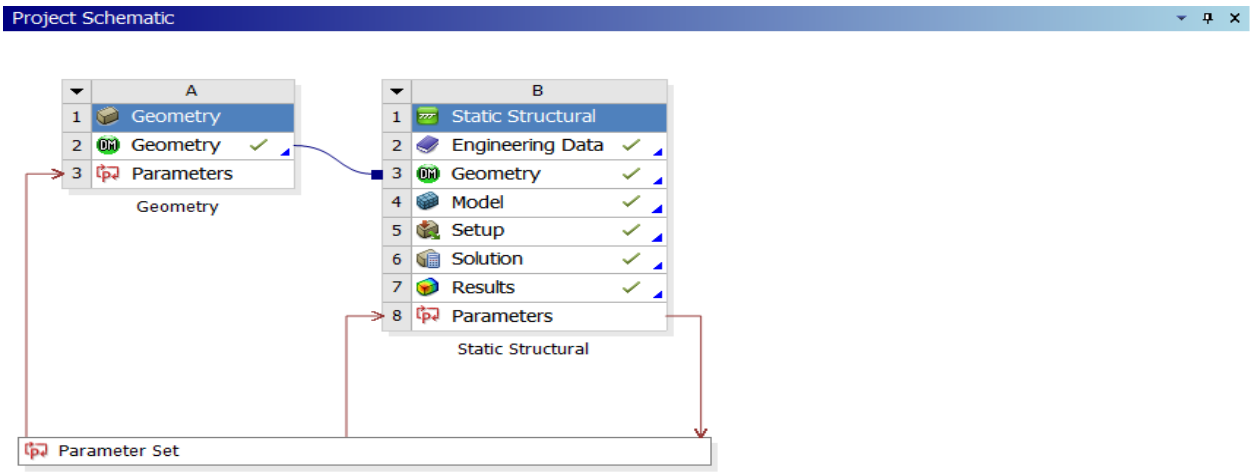

Figure 60 Project schematic for static structural analysis

The geometry in ANSYS Workbench shows in Fig 60.

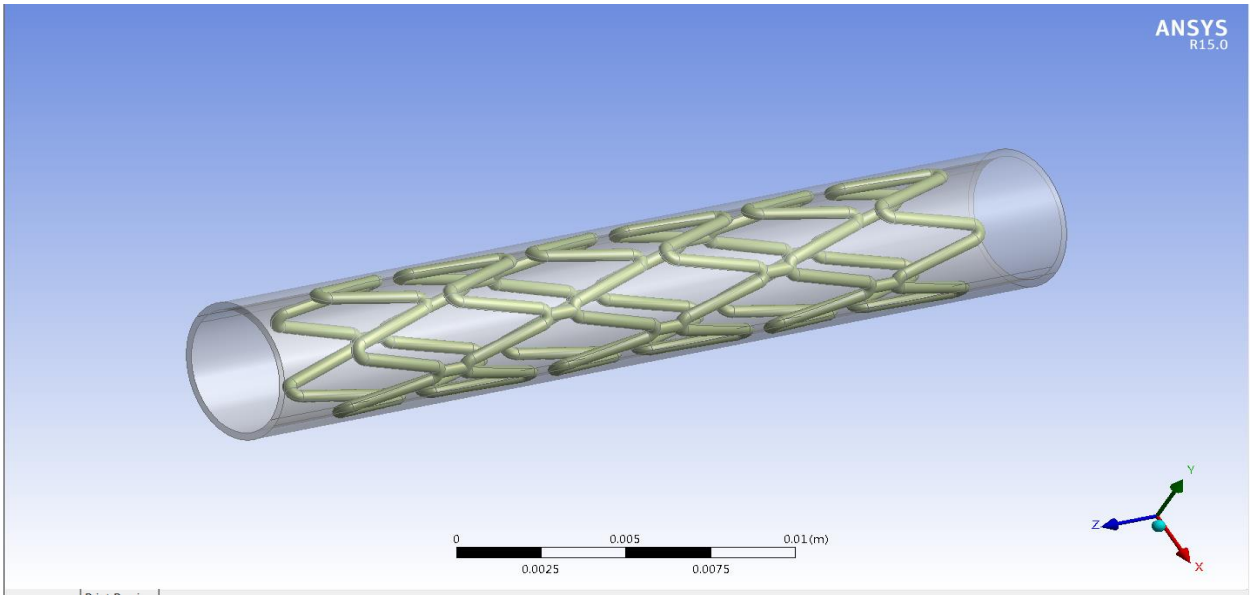

Figure 61 Geometry in ANSYS Workbench

In the simulation, the concept of contact and target surfaces are used for each contact region (Figure 61). One side of the contact region is comprised of "contact" faces, and the other side of the region is made of "target" faces. Based on the fact that biodegradable stents expand to and support the blood vessel, the "bonded" contact type is selected in this project, which is basically linear behavior.

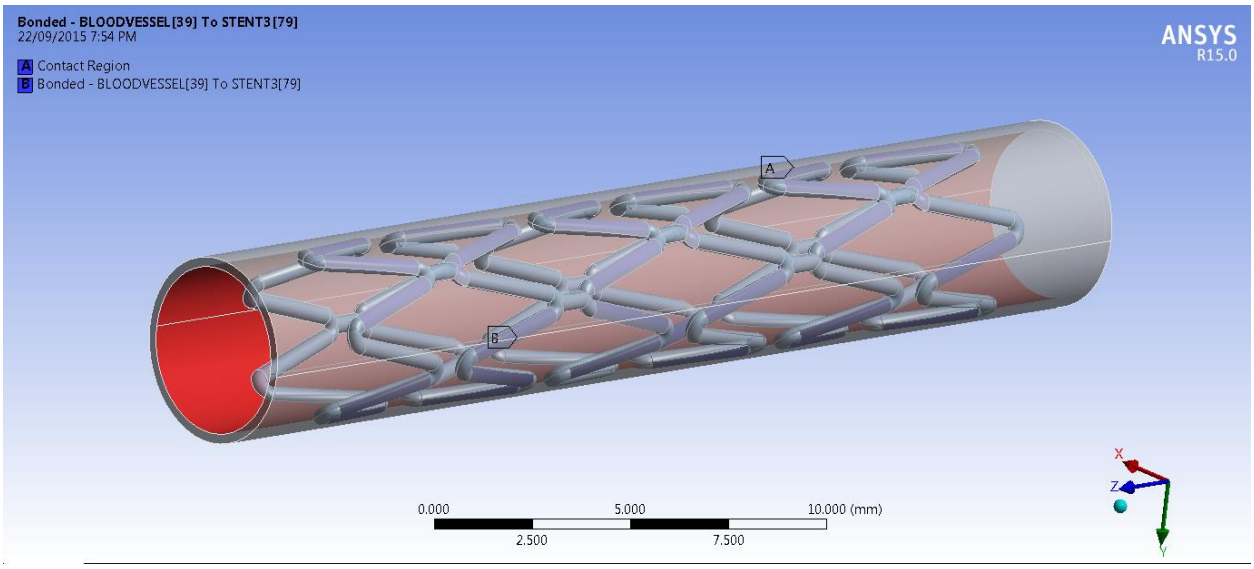

Figure 62 Contact region between blood vessel and biodegradable stents

The mesh cells are mixed with hexahedron and tetrahedron cells. Hexahedrons can fill a given volume more efficiently than other mesh shapes, and additionally,hexahedron meshes are more uniform. But if hexahedron can not sweep a body, it is free meshed with tetrahedral elements. There are 21652 nodes and 8817 elements totally in Figure 62.

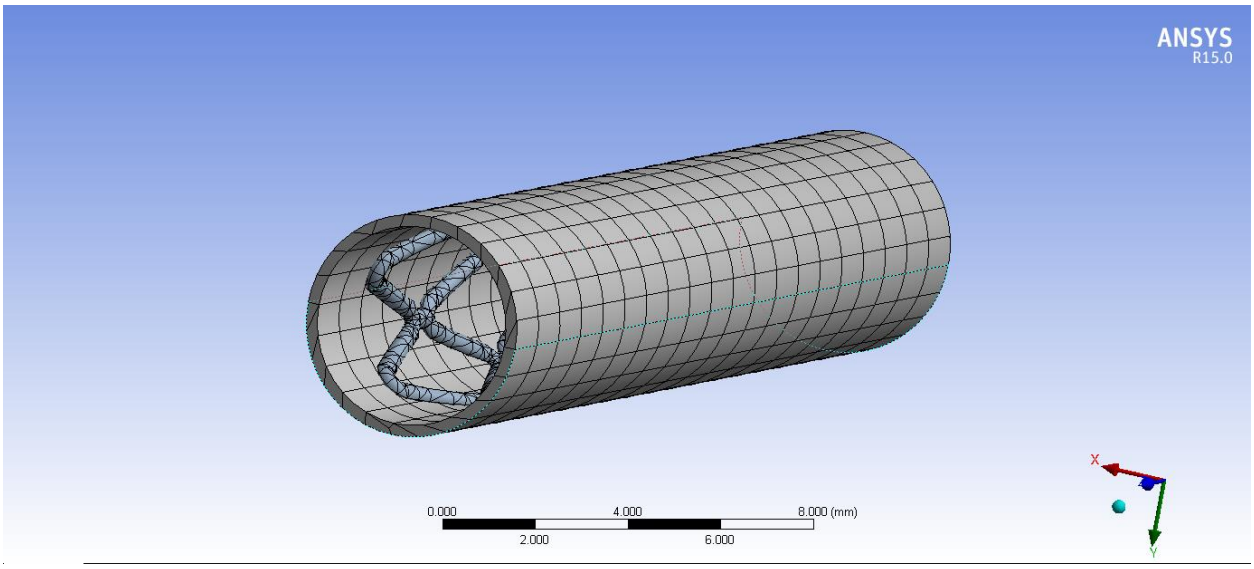

Figure 63 Mesh modeling

6.3.2 Material properties

Material input is under the "Engineering Data" branch, and material assignments are per part under the "Geometry" branch. The required structural material properties are young's modulus and Poisson's ratio for linear static structural analyzes (Figure 63). The stent is made of PCL whose young modulus is 400 Mpa, and the Poisson ratio is 0.33 [55]. While the Young' modulus of the blood vessel is 0.45 Mpa, and the Poisson ratio is 0.45 [62].

Outline of Schematic B2: Engineering Data

	A	B	C	D
1	Contents of Engineering Data		ourc	Description
2	Material			
3	Structural Steel			Fatigue Data at zero mean stress comes from 1998 ASME BPV Code, Section 8, Div 2, Table 5-110.1
4	Stent			
5	BloodVessel			
*	Click here to add a new material			

Properties of Outline Row 3: bloodvessel

	A	B	C	D	E
1	Property	Value	Unit		
2	Density	1150	kg m^-3		
3	Isotropic Elasticity				
4	Derive from	Young's Modulus and P...			
5	Young's Modulus	4.5E+05	Pa		
6	Poisson's Ratio	0.45			
7	Bulk Modulus	1.5E+06	Pa		
8	Shear Modulus	1.5517E+05	Pa		

Properties of Outline Row 4: stent

	A	B	C	D	E
1	Property	Value	Unit		
2	Density	1140.8	kg m^-3		
3	Isotropic Elasticity				
4	Derive from	Young's Modulus and P...			
5	Young's Modulus	400	MPa		
6	Poisson's Ratio	0.33			
7	Bulk Modulus	3.9216E+08	Pa		
8	Shear Modulus	1.5038E+08	Pa		

Figure 64 Material properties for blood vessel and biodegradable stents

6.3.3 Loading and Boundary conditions

Pressures can only be applied to surfaces and always at normal to the surface. Positive value acts into the surface, and negative value acts outward from the surface. To simulate the vasoconstriction, the pressure is applied on internal surface is (P1) -1.2e-002 Mpa (or 90 mm Hg), which is the average blood pressure in the human body (Figure 64).

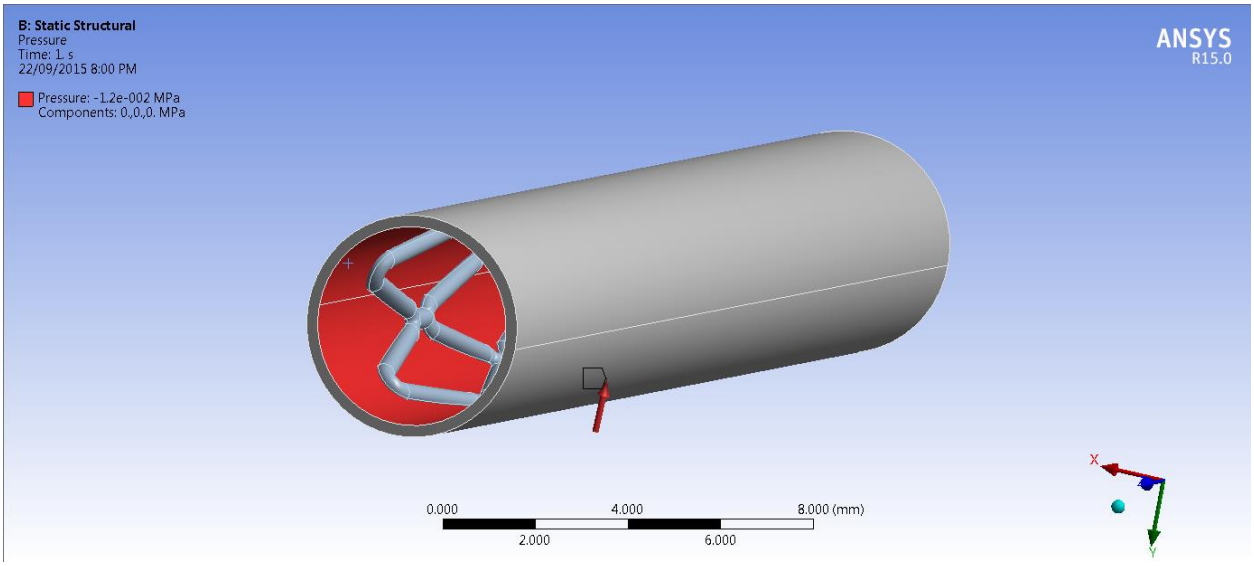

Figure 65 Pressure on the blood vessel

The fixed support constraints all degrees of freedom on vertex, edge, or surface, which prevents translations and rotations in X, Y and Z. The fixed supports are applied on the both sides of a blood vessel (Figure 65).

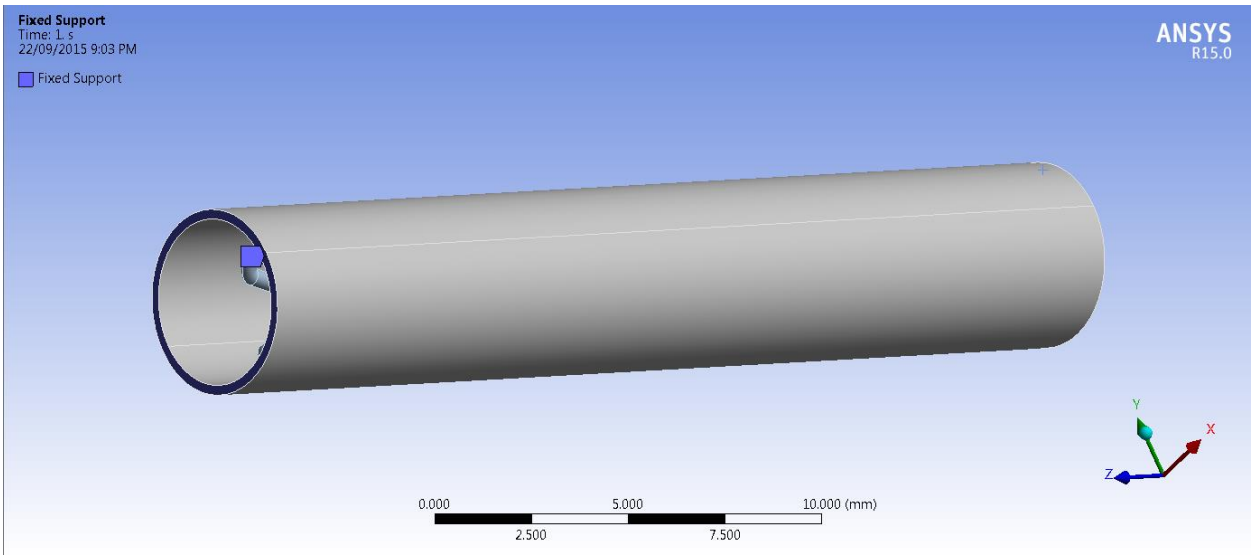

Figure 66 Fixed support on the both sides of blood vessel

6.3.4 Results

The solution obtained from the FEA estimates the exact natural solution (Figure 66).

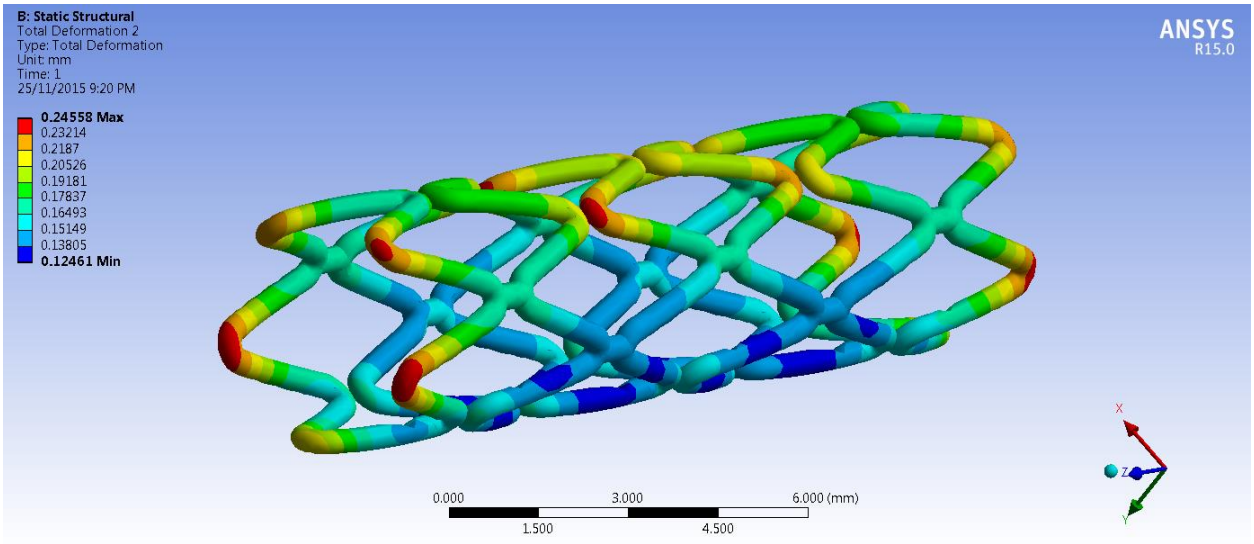

Figure 67 The total deformation of biodegradable stents

The blood vessel pressure is 1.2e-002 Mpa, which makes the biodegradable stent in the region of elastic deformation. Radial deformation can be observed in the stents as a result of the radially compressive forces exerted by the artery. The rigidity of biodegradable stents can resist the elastic recoil of the vessel wall, which can be calculated by $\Delta D/D_0$: 0.24558/3.4=7.22% while the elastic recoil of metallic stents is from 3.7% to 12.8% with the compressive pressures between 0.7 to 20 atm [63]. The result shows that the rigidity of biodegradable stents is still a little weaker than metallic stents.

6.4 Conclusions

The total deformation of biodegradable stents in blood vessel shows that the rigidity of biodegradable stents is still a little weaker than metallic stents. The maximum stress happened on the apex of the stent. A finite element analysis similar to the one herewith proposed could help in designing new structure of stents or analyzing actual stents to ensure enough mechanical property.

CHAPTER 7 Conclusions and Future work

7.1 Conclusions

This thesis presented a study toward fabrication and optimal design of biodegradable stents for aneurysms treatment. The study focused on developing methods to fabricate the biodegradable stents and optimizing the structure of biodegradable stents with an aim to obtain a minimum radial deformation in the blood vessel. The major findings of this research are summarized as follows.

1. The technique of dispensing-based rapid prototyping (DBRP) allowing more accurate control over the scaffold microstructure is promising to facilitate the fabrication of stents as designed.
2. The radial deformation of the biodegradable stent can be characterized by an precise compression test system. The biodegradable stents with highest radial stiffness in nine groups can be obtained by comparing the forces required to compress stents radially from 10% to 40%.
3. The parametric 3D model of biodegradable stents can be built by Pro/Engineer, and the simulation of actual compression test can be performed by a static structural analysis through ANSYS Workbench. The comparison results between simulation and actual compression test show that the finite element model of biodegradable stents is acceptable within the range of around 20% radial deformation.
4. The results of optimization of biodegradable stents present that the total deformation can be decreased by 35.82% (from 0.589 mm to 0.378 mm) by modifying the parameters of the geometry, which makes a significant contribution to increasing the radial stiffness of biodegradable stents.
5. The total deformation of optimized biodegradable stents in the blood vessel is 0.25 mm in the simulation, and the rigidity of biodegradable stents is 7.22%, which can support the blood vessel wall. Although the result still shows that the rigidity of biodegradable stents is weaker than metallic stents, the finite element analysis could help in designing new stents or analyzing actual stents to ensure enough mechanical property.

7.2 Future Work

Several future endeavors could potentially improve upon this thesis work.

First, the finite element model of biodegradable stents in this thesis is linear, while a more accurate model for predicting the force VS deformation in the large deformation region is nonlinear, which can be improved with a more precise acquisition of the nonlinear plastic material properties and structure modelling.

Second, it is important to model the degradation and time-dependent behavior of biodegradable stents, as the mechanical properties of biodegradable stents are highly dependent on the process of degradation in the human body. It is a challenge to design a biodegradable stent providing structural support for an appropriate time to facilitate the blood vessel healing.

Finally, with an aim of verifying the deformation of biodegradable stents in the blood vessel in the simulation, the data of the deformation of the biodegradable stents in vivo test is needed.

Reference

1. National Heart,Lung and Blood Institue, *"What Is an Aneurysm?."* April 1, 2011. Web.27 Jan 2016.
2. Keedy, A., *An overview of intracranial aneurysms*. McGill Journal of Medicine: MJM, 2006. 9(2): p. 141..
3. Lubicz, B., *Frontiers of stent-assisted aneurysm coiling.* Neuroradiology, 2011. **53**(12): p. 937-938.
4. Erne, P., M. Schier, and T.J. Resink, *The road to bioabsorbable stents: reaching clinical reality?* Cardiovascular and interventional radiology, 2006. 29(1): p. 11-16.
5. Pinto Slottow, T.L. and R. Waksman, *Overview of the 2006 Food and Drug Administration Circulatory System Devices Panel meeting on drug‐eluting stent thrombosis.* Catheterization and Cardiovascular Interventions, 2007. 69(7): p. 1064-1074.
6. Eury, R.P., *Multilayered biodegradable stent and method of manufacture.* European Patent Application EP0604022, Kind Code:A1, 1995.
7. Hermawan, H., D. Dubé, and D. Mantovani, *Developments in metallic biodegradable stents.* Acta biomaterialia, 2010. **6**(5): p. 1693-1697.
8. Colombo, A. and E. Karvouni, Biodegradable stents: *"fulfilling the mission and stepping away"*. Circulation, 2000. 102(4): p. 371-373.
9. Werner, M., et al., *Evaluation of the biodegradable peripheral Igaki-Tamai stent in the treatment of de novo lesions in the superficial femoral artery: the GAIA study.* JACC: Cardiovascular Interventions, 2014. **7**(3): p. 305-312.
10. Kwon, D.Y., et al., *Biodegradable stent.* 2012.
11. Muramatsu, T., et al., *Progress in treatment by percutaneous coronary intervention: the stent of the future.* Revista Española de Cardiología (English Edition), 2013. **66**(6): p. 483-496.
12. Waksman, R., *Biodegradable stents: they do their job and disappear.* The Journal of invasive cardiology, 2006. **18**(2): p. 70-74.
13. AGRAWAL, C.M. and H.G. CLARK, *Deformation characteristics of a bioabsorbable intravascular stent.* Investigative radiology, 1992. **27**(12): p. 1020-1023.
14. Li, M., X. Tian, and X. Chen, *A brief review of dispensing-based rapid prototyping techniques in tissue scaffold fabrication: role of modeling on scaffold properties prediction.* Biofabrication, 2009. **1**(3): p. 032001.
15. Chen, X., M. Li, and H. Ke, *Modeling of the flow rate in the dispensing-based process for fabricating tissue scaffolds.* Journal of Manufacturing Science and Engineering, 2008. **130**(2): p. 021003.
16. Pierot, L. and A.K. Wakhloo, *Endovascular treatment of intracranial aneurysms current status. Stroke*, 2013. 44(7): p. 2046-2054.Silva, G.S., et al., Causes of Ischemic Stroke, in Acute Ischemic Stroke, 2011, Springer. p. 25-42.

17. Wanke, I. and M. Forsting, *Stents for intracranial wide-necked aneurysms: more than mechanical protection.* Neuroradiology, 2008. 50(12): p. 991-998.
18. Ogilvy, C.S., et al., *Stent-assisted coiling of paraclinoid aneurysms: risks and effectiveness*. Journal of neurointerventional surgery, 2010: p. jnis. 2010.002303.
19. Waksman, R. and R. Pakala, *Biodegradable and bioabsorbable stents.* Current pharmaceutical design, 2010. **16**(36): p. 4041-4051.
20. Eberhart, R.C., et al., *Review: Bioresorbable polymeric stents: current status and future promise.* Journal of Biomaterials Science, Polymer Edition, 2003. **14**(4): p. 299-312.
21. Onuma, Y. and P.W. Serruys, *Bioresorbable Scaffold The Advent of a New Era in Percutaneous Coronary and Peripheral Revascularization?* Circulation, 2011. **123**(7): p. 779-797.
22. Mathew, A.P., K. Oksman, and M. Sain, *Mechanical properties of biodegradable composites from poly lactic acid (PLA) and microcrystalline cellulose (MCC).* Journal of Applied Polymer Science, 2005. **97**(5): p. 2014-2025.
23. Serrano, M., et al., *In vitro biocompatibility assessment of poly (ε-caprolactone) films using L929 mouse fibroblasts.* Biomaterials, 2004. **25**(25): p. 5603-5611.
24. Strohbach, A. and R. Busch, *Polymers for Cardiovascular Stent Coatings.* International Journal of Polymer Science, 2015. **2015**.
25. Nair, L.S. and C.T. Laurencin, *Biodegradable polymers as biomaterials.* Progress in Polymer Science, 2007. **32**(8): p. 762-798.
26. Zilberman, M. and R. C. Eberhart (2006). "*Drug-eluting bioresorbable stents for various applications*." Annu. Rev. Biomed. Eng. 8: 153-180.
27. Yaszemski, M.J., et al., *Tissue engineering and novel delivery* systems, 2003: CRC Press.
28. Woodruff, M.A. and D.W. Hutmacher, *The return of a forgotten polymer—polycaprolactone in the 21st century.* Progress in Polymer Science, 2010. **35**(10): p. 1217-1256
29. Ajili, S.H., N.G. Ebrahimi, and M. Soleimani, *Polyurethane/polycaprolactane blend with shape memory effect as a proposed material for cardiovascular implants.* Acta biomaterialia, 2009. **5**(5): p. 1519-1530.
30. Rogers, C. and E.R. Edelman, *Endovascular stent design dictates experimental restenosis and thrombosis.* Circulation, 1995. 91(12): p. 2995-3001.
31. Su, S.-H. and R.C. Eberhart, *Expandable biodegradable polymeric stents for combined mechanical support and pharmacological or radiation therapy*, 2006, Google Patents.
32. Wikipedia contributors. "*Zigzag*." Wikipedia, The Free Encyclopedia. Wikipedia, The Free Encyclopedia, 12 Apr. 2015. Web. 28 Jan. 2016.
33. Luehrs, K.F., *Flexible stent*, 2001, Google Patents.
34. Erne, P., M. Schier, and T.J. Resink, *The road to bioabsorbable stents: reaching clinical reality?* Cardiovascular and interventional radiology, 2006. **29**(1): p. 11-16.
35. Tamai, H., et al., *Initial and 6-month results of biodegradable poly-l-lactic acid coronary stents in humans.* Circulation, 2000. **102**(4): p. 399-404.

36. Van Ditzhuijzen, N.S., et al., *Bioabsorbable Stent*, in *Cardiovascular OCT Imaging*2015, Springer. p. 179-193.
37. Onuma Y, Serruys PW, Ormiston JA, Regar E, Webster M, Thuesen L, et al. *Three-year results of clinical follow-up after a bioresorbable everolimus-eluting scaffold in patients with de novo coronary artery disease: the ABSORB trial*. EuroIntervention. 2010;6:447–53.
38. Onuma, Y. and P.W. Serruys, *Bioresorbable Scaffold The Advent of a New Era in Percutaneous Coronary and Peripheral Revascularization?* Circulation, 2011. **123**(7): p. 779-797.
39. Ormiston, J.A. and P.W. Serruys, *Bioabsorbable coronary stents.* Circulation: Cardiovascular Interventions, 2009. **2**(3): p. 255-260.
40. Alexy, R.D. and D.S. Levi, *Materials and manufacturing technologies available for production of a pediatric bioabsorbable stent.* BioMed research international, 2013. **2013**.
41. Martinez, A.W. and E.L. Chaikof, *Microfabrication and nanotechnology in stent design.* Wiley Interdisciplinary Reviews: Nanomedicine and Nanobiotechnology, 2011. **3**(3): p. 256-268.
42. Park, J.-H., et al. *Micromachined biodegradable microstructures*. in *Micro Electro Mechanical Systems, 2003. MEMS-03 Kyoto. IEEE The Sixteenth Annual International Conference on*. 2003. IEEE.
43. Armani, D.K. and C. Liu. *Microfabrication technology for polycaprolactone, a biodegradable polymer*. in *Micro Electro Mechanical Systems, 2000. MEMS 2000. The Thirteenth Annual International Conference on*. 2000. IEEE.
44. Lafont, A., et al., *PLA stereocopolymers as sources of bioresorbable stents: Preliminary investigation in rabbit.* Journal of Biomedical Materials Research Part B: Applied Biomaterials, 2006. **77**(2): p. 349-356.
45. Ryu, W., et al., *Microfabrication technology of biodegradable polymers for interconnecting microstructures.* Microelectromechanical Systems, Journal of, 2006. **15**(6): p. 1457-1465.
46. Chiang, W., et al., *Application of rapid prototyping and tooling in customised airway management.* Rapid Prototyping Journal, 2005. 11(2): p. 106-112.
47. Mori, K. and T. Saito, *Effects of stent structure on stent flexibility measurements*. Annals of biomedical engineering, 2005. 33(6): p. 733-742.
48. Rieu, R., et al., *Radial force of coronary stents: a comparative analysis*. Catheterization and Cardiovascular Interventions, 1999. 46(3): p. 380-391.
49. Rieu, R., et al., *Radial force of coronary stents: a comparative analysis*. Catheterization and Cardiovascular Interventions, 1999. 46(3): p. 380-391.
50. Baumgart, F., *Stiffness-an unknown world of mechanical science?* Injury-International Journal for the Care of the Injured, 2000. **31**(2): p. 14-23.

51. Enkatesh, B., V. Kamala, and P. AMK, *Modeling and Analysis of Aluminum A360 Alloy Helical Gear for Marine Applications.* International Journal of Applied Engineering Research, Dindigul, 2010. **1**(2): p. 124-134.
52. Zienkiewicz, O.C. and R.L. Taylor, *The finite element method for solid and structural mechanics*, 2005: Butterworth-heinemann.
53. Lee, H.-H., *Finite element simulations with ANSYS Workbench 14*2012: SDC publications
54. Awang, M., E. Mohammadpour, and I.D. Muhammad, *Finite Element Modeling of Nanotube Structures: Linear and Non-linear* Models, 2015: Springer.
55. Hughes, T.J., *The finite element method: linear static and dynamic finite element analysis*2012: Courier Corporation.D. C. Montgomery, *Design and Analysis of Experiments*, Hoboken, NJ: John Wiley and Sons, 2009.
56. Fang, Z., B. Starly, and W. Sun, *Computer-aided characterization for effective mechanical properties of porous tissue scaffolds.* Computer-Aided Design, 2005. **37**(1): p. 65-72.
57. ANSYS, "*Meshing Methods: Tetrahedral*." Web. 27 Jan. 2016.
58. ANSYS, Inc., "*ANSYS Parametric Design Language Guide"*, April 2009. Available: http://www.ansys.com. April, 2012.
59. L'italien, G.J., et al., *In vivo measurement of blood vessel wall thickness.* American Journal of Physiology-Heart and Circulatory Physiology, 1979. **237**(2): p. H265-H268.
60. ANSYS, "*Introduction to ANSYS."* Web. 27 Jan. 2016.
61. ANSYS, "*ANSYS DesignXplorer.".* Web. 27 Jan. 2016.
62. Oscuii, H. Niroomand; Shadpour, M. Tafazzoli and Ghalichi, *Flow Characteristics in Elastic Arteries Using a Fluid-Structure Interaction Mode*. American Journal of Applied Sciences, 2007, Vol. 4 Issue 8, p. 516
63. Etave, F., et al., *Mechanical properties of coronary stents determined by using finite element analysis.* Journal of Biomechanics, 2001. **34**(8): p. 1065-1075.